DUDLEY KNOX LIBRARY
NAVAL POSTGRADUATE SCHOOL
MONTEREY, CALIF. 93940

NAVAL POSTGRADUATE SCHOOL
Monterey, California

THESIS

VALIDATION OF A TWO-DIMENSIONAL PRIMITIVE VARIABLE COMPUTER CODE FOR FLOW FIELDS IN JET ENGINE TEST CELLS

by

Paul Joseph Mallon

June 1980

Thesis Advisor: D. W. Netzer

Approved for public release; distribution unlimited

T196280

SECURITY CLASSIFICATION OF THIS PAGE (When Data Entered)

REPORT DOCUMENTATION PAGE

READ INSTRUCTIONS BEFORE COMPLETING FORM

1. REPORT NUMBER

2. GOVT ACCESSION NO.

3. RECIPIENT'S CATALOG NUMBER

4. TITLE (and Subtitle)

Validation of a Two-Dimensional Primitive Variable Computer Code for Flow Fields in Jet Engine Test Cells

5. TYPE OF REPORT & PERIOD COVERED

Master's Thesis; June 1980

6. PERFORMING ORG. REPORT NUMBER

7. AUTHOR(s)

Paul Joseph Mallon

8. CONTRACT OR GRANT NUMBER(s)

9. PERFORMING ORGANIZATION NAME AND ADDRESS

Naval Postgraduate School
Monterey, California 93940

10. PROGRAM ELEMENT, PROJECT, TASK AREA & WORK UNIT NUMBERS

N6237680WR00009

11. CONTROLLING OFFICE NAME AND ADDRESS

Naval Air Propulsion Center
Trenton, NJ

12. REPORT DATE

June 1980

13. NUMBER OF PAGES

75

14. MONITORING AGENCY NAME & ADDRESS(if different from Controlling Office)

Naval Postgraduate School
Monterey, California 93940

15. SECURITY CLASS. (of this report)

Unclassified

15a. DECLASSIFICATION/DOWNGRADING SCHEDULE

16. DISTRIBUTION STATEMENT (of this Report)

Approved for public release; distribution unlimited.

17. DISTRIBUTION STATEMENT (of the abstract entered in Block 20, if different from Report)

18. SUPPLEMENTARY NOTES

19. KEY WORDS (Continue on reverse side if necessary and identify by block number)

Primitive Variable Computer Model
Jet Engine Test Cell

20. ABSTRACT (Continue on reverse side if necessary and identify by block number)

Pressure and velocity data were collected in a full scale jet engine test cell in order to validate the predictive accuracy of a two-dimensional and axisymmetric primitive variable computer code. It was found that the model reasonably predicted the velocity profiles in the augmentor tube. Inaccuracy increased at higher engine thrust settings at positions far downstream in the augmentor tube. Predicted pressure profiles were reasonable but the magnitudes were in considerable error at high flow rates.

DD FORM 1 JAN 73 1473 EDITION OF 1 NOV 65 IS OBSOLETE
S/N 0102-014-6601

(Page 1)

SECURITY CLASSIFICATION OF THIS PAGE (When Data Entered)

Approved for public release; distribution unlimited.

Validation of a Two-Dimensional Primitive Variable Computer Code for Flow Fields in Jet Engine Test Cells

by

Paul Joseph Mallon
Lieutenant, United States Navy
B.S., Tulane University, 1971

Submitted in partial fulfillment of the
requirements for the degree of

MASTER OF SCIENCE IN AERONAUTICAL ENGINEERING

from the

NAVAL POSTGRADUATE SCHOOL
June 1980

DUDLEY KNOX LIBRARY
NAVAL POSTGRADUATE SCHOOL
MONTEREY, CALIF 93940

ABSTRACT

Pressure and velocity data were collected in a full scale jet engine test cell in order to validate the predictive accuracy of a two-dimensional and axisymmetric primitive variable computer code. It was found that the model reasonably predicted the velocity profiles in the augmentor tube. Inaccuracy increased at higher engine thrust settings at positions far downstream in the augmentor tube. Predicted pressure profiles were reasonable but the magnitudes were in considerable error at high flow rates.

TABLE OF CONTENTS

		PAGE NO.
I.	INTRODUCTION	10
II.	EXPERIMENTAL INVESTIGATION	14
	A. Introduction	14
	B. Test Cell	15
	C. Instrumentation and Data Acquisition	16
	D. Experimental Procedure	18
	E. Data Reduction	25
III.	COMPUTER MODEL	29
	A. Introduction	29
	B. Physical Model	29
	C. Data Input	31
IV.	DISCUSSION OF RESULTS	34
	A. Introduction	34
	B. Experimental Data	34
	C. Computer Model Predictions	36
V.	CONCLUSIONS AND RECOMMENDATIONS	41
LIST OF REFERENCES		74
INITIAL DISTRIBUTION LIST		75

LIST OF TABLES

		PAGE NO.
I.	Thermocouple Data Obtained During Initial Engine Testing	19
II.	Experimental Data, 100% Power	22
III.	Experimental Data, 90% Power	23
IV.	Experimental Data, Idle Power	24
V.	Velocimeter Data	26
VI.	Computer Input Data	33

LIST OF FIGURES

		PAGE NO.
1.	TF-34 Test Configurations	42
2.	Pitot Rake Front View	43
3.	Pitot Rake Mounted in Augmentor Tube	44
4.	Pitot Rake Construction	45
5.	Rake Attachment	46
6.	Instrumentation	47
7.	Velocimeter Calibration Curves	48
8.	Pitot Tube/Thermocouple Labels	49
9.	Static Port Labels	49
10.	Pressure Profile, Idle Power	50
11.	Pressure Profile, 90% Power	51
12.	Pressure Profile, 100% Power	52
13.	Stagnation Temperature Profiles, Aft Rake	53
14.	Static Temperature Profiles, Aft Rake	54
15.	Velocity Profile, Aft Rake, Idle Power	55
16.	Velocity Profile, Aft Rake, 90% Power	56
17.	Velocity Profile, Aft Rake, 100% Power	57
18.	Stagnation Temperature Profiles, Forward Rake	58
19.	Velocity Profile, Forward Rake, Idle Power	59
20.	Velocity Profile, Forward Rake, 90% Power	60
21.	Velocity Profile, Forward Rake, 100% Power	61
22.	Turbojet Test Cell Geometry for Computer Model	62
23.	TF-34 Exhaust	63

PAGE NO.

24. Computer Model of TF-34 Exhaust Velocity Profile ------- 64

25. Average Velocity Profiles, Aft Rake ------------------- 65

26. Modified Stagnation Temperature Profile, Aft Rake, 90% Power -- 66

27. Sensitivity of Velocity Profile to Uncertainties in Measured Static Pressure, 90% Power ------------------- 67

28. Sensitivity of Predicted Velocity Profile to Test Cell Mass Flow Rate, 90% Power ------------------------------ 68

29. Sensitivity of Predicted Static Pressure Profile to Test Cell Mass Flow Rate, 90% Power ------------------- 69

30. Sensitivity of Predicted Velocity Profile to a 50% Increase in Effective Viscosity, 90% Power ------------ 70

31. Sensitivity of Predicted Pressure Profile to a 50% Increase in Effective Viscosity, 90% Power ------------ 71

32. Sensitivity of Predicted Velocity Profile to a 33% Decrease in Effective Viscosity, 90% Power ------------ 72

33. Sensitivity of Predicted Pressure Profile to a 33% Decrease in Effective Viscosity, 90% Power ------------ 73

LIST OF SYMBOLS

ROMAN SYMBOLS

H_g	Mercury
K	Turbulence kinetic energy
M	Mach number
p	Pressure
RPM	Revolutions per minute
T	Temperature
u	Axial velocity
v	Radial velocity

GREEK SYMBOLS

γ	Specific heat ratio
ε	Turbulence dissipation rate
μ	Viscosity
ψ	Stream function
ω	Vorticity

SUBSCRIPTS

cell	Any condition in the test cell
T	Stagnation property

ACKNOWLEDGEMENT

I would like to take this opportunity to thank Professor David W. Netzer, Mr. Patrick J. Hickey, and the men of the NARF Alameda. Professor Netzer's help and patience over the course of this investigation proved invaluable. Mr. Hickey's technical expertise provided the backbone for the data collection phase of this report. All the men of NARF Alameda associated with the investigation, but especially Mr. Glenn Evans, Mr. Paul Mullaly, and Mr. Luther McCoy were most cooperative and helpful at all times.

I. INTRODUCTION

Jet engine test cells are in wide use today in military and commercial aviation maintenance programs. Their purpose is to provide for testing of jet engines under conditions that approximate the installed environment, thus enabling the responsible authority to verify the engine's capabilities throughout its operational envelope prior to returning it to service. However, due to exhaust pollution problems inherent to their operation, the use of these test facilities has recently encountered a considerable amount of criticism and even judicial action in the State of California.

The necessity for testing an engine after overhaul is apparent. However, the pollution problems that result when testing today's high power, high mass flow engines in present test facilities must also be considered.

"The typical test cell incorporates an inlet, a horizontal test section and vertical exhaust stack. The engine to be tested is normally mounted near the center of the cell to allow the development of a nearly uniform engine inlet velocity profile. The engine exhausts into an augmentor tube which entrains additional air for exhaust gas cooling and dilution. The quantity of this secondary air is crucial to proper engine testing and test cell performance" [Ref. 1]. The ratio of entrained air mass flow rate to engine mass

flow rate is known as "augmentation ratio". An augmentation ratio that is too high could result in inaccurate engine performance measurements and in exceeding the test cell structural limits due to pressure gradients and excessive cell pressure reduction. Insufficient secondary air could allow engine exhaust gas recirculation to the engine inlet and cause excessive opacity of visible emittants. It is therefore necessary to develop mathematical models which can be used to predict the flow fields within turbojet test cells. These models could then be used as a cost effective means for determination of optimum test cell designs for meeting the military engine testing needs while minimizing noise and chemical pollution effects on the local environment.

With this in mind, considerable experimental and computer modelling work has been done at the Naval Postgraduate School to further the understanding of the flow field and detailed operating characteristics encountered in typical test cells. This knowledge is currently needed to facilitate the necessary modifications to present test cells and for the design of new cells to accommodate the high technology engines of the future.

The two-dimensional modelling of the flow within turbojet test cells was initiated at NPS by Hayes and Netzer [Ref. 2]. They adapted the two-dimensional, ψ-ω model of Spalding, et al [Refs. 3, 4] to the test cell geometry and operating conditions. This work was continued by Speakman, Hayes and Netzer [Ref. 5]. The model made use of the fundamental equations of conservation of mass, momentum and energy. The dependent variables were stream functions (ψ), vorticity (ω),

turbulence kinetic energy (K), the turbulence dissipation rate (ε), and the temperature (T). As a consequence of the ψ-ω formation, pressure (and to a large extent velocity) is removed from the governing equations. These second order elliptic partial differential equations were reduced to "finite-difference," non-linear algebraic equations and solved simultaneously with an iterative procedure. Results of this computer simulation appeared to be quite accurate at low subsonic engine exhaust Mach numbers ($M < 0.6$), but pressure predictions were unreliable at high subsonic or sonic exhaust velocities. These comparisons between predictions and experiment were made by Walters and Netzer [Ref. 6] using a one eighth scale model of an NAS Alameda test cell. Other problems related to the ψ-ω formulation were: 1) restriction to constant density flows, or to flows in which density varied only with temperature; 2) boundary conditions were difficult to specify; 3) considerable difficulty was experienced in obtaining converged solutions, especially for non-uniformly spaced grids and high flow rates, and 4) the ψ-ω model is not easily extended to three dimensional flows.

To help alleviate the above modelling difficulties Stevenson and Netzer [Ref. 1] utilized a primitive variable (pressure-velocity) model. This computer model (adapted from the CHAMPION 2/E/FIX computer program developed by Pun and Spalding [Ref. 7] extended the modelling capabilities to more complex geometries and to high subsonic and sonic engine exhaust velocities. It also is readily applicable to variable density flows. The earlier results of the ψ-ω model and those of the u-v-p model were compared to the empirical data obtained with the subscale test cell [Ref. 6]. Good agreement between the two methods was found

for low subsonic engine exhaust conditions. The primitive variable computer model produced reasonable results for the flow field downstream of the engine exhaust up to the sonic exhaust condition.

The primary objective of this investigation was to adapt Spalding's CHAMPION 2/E/FIX primitive variable computer model (as modified by Stevenson) to the geometry and flow conditions of an actual operational full scale turbojet test cell and to test that model with empirical data from the same cell. The turbojet test cell chosen was one located at NAS Alameda, operated by NARF Alameda. The engine being operated at the time of data acquisition was the General Electric TF34-GE-100, currently used on the USAF A-10 attack aircraft. The major computer model modifications required were: 1) to increase the geometry to the full scale, and 2) to change the uniform engine exhaust velocity profile to a non-uniform profile which adequately represented the primary and secondary flows from the TF-34 turbofan engine.

II. EXPERIMENTAL INVESTIGATION

A. INTRODUCTION

The turbojet test cell chosen for this investigation was test cell No. 13 located in Building 372 at NAS Alameda. It is operated by NARF Alameda as the prime means of evaluating the USAF TF34-GE-100 turbofan engine following required normal periodic maintenance.

The TF34-GE-100 is a turbofan engine in current use on the USAF twin engine A-10 attack airplane. The engine is 2.54m long and produces a maximum rated thrust of 9065 lbf [Ref. 8]. The bypass ratio is 6.22:1 with maximum rated airflow at 151.0 kg/sec. The exhaust nozzle is a fixed area, convergent type with the cold stream being 0.474 sq. m. in area and the hot stream 0.148 sq. m. in area. While operating at maximum power the core exhaust gas is estimated to have a velocity of 305 m/sec and a temperature of 393°C [Ref. 8].

To provide the data for model validation it was decided to measure velocity profiles within the test cell and at two locations within the augmentor tube as well as the axial pressure distribution throughout the test cell. To most accurately determine velocity profiles, multiple pitot-static tubes with associated stagnation temperature measurements would have been required. However, due to cost and time restraints involved with the manufacturing and installation of such equipment, a compromise approach to this problem was taken. Two stagnation tube rakes, each fitted with two thermocouples, were installed in the augmentor tube. Also, thirty two static pressure ports were installed in the augmentor tube wall. Velocity measurements were also made within

the test cell using hot wire velocimeters. Details of the data acquisition as well as the method of data reduction are presented below.

B. TEST CELL

The turbojet test cell utilized in this investigation is typical of test cells currently used in military and commercial aviation maintenance programs. It was a concrete blockhouse type structure 43m long, 9m high, and 9m wide (Fig. 1). It had a horizontal inlet, which was retangular in cross section, and exhausted into a vertical stack. Not shown in Figure 1 are the noise suppression devices which were located over the cross sections of both the test cell inlet and back wall. Located 15m from the cell inlet was the test platform which stood 3m above the floor of the cell. The jet engine test stand and the first section of the augmentor tube were located on this platform. The TF-34 was mounted on the test stand with an attached, fixed geometry bellmouth type inlet, along with necessary start-up and test equipment to monitor engine performance in the cell control room. This test stand was movable, so that the distance between the exit plane of the engine and entrance plane of the augmentor tube could be varied. During this investigation this distance was fixed at 1.7m.

The first section of the augmentor tube was located on the test platform. As shown in Figure 1 it too was movable. It was a steel pipe with 9.5mm thick walls and was approximately 1.8m in diameter and 1.6m long. The next section was also a constant diameter pipe, 5.2m long. During this investigation, the pipe protruded only 5m beyond the first section. The radial gap between these two sections was, on the average, 16mm. The next section was 3.5m long and diverged in

diameter from approximately 1.8m to 2.7m. At the downstream end of the latter section was a water-injection ring. Following a 0.31m gap was the next section: a constant 3.05m diameter pipe, 13.1m long. In this section were three staggered rows of four noise suppression devices. Each unit was a 3.2m long cylinder, 0.6m in diameter.

C. INSTRUMENTATION AND DATA ACQUISITION

Two pitot tube rakes were utilized in this investigation. Each rake was constructed from 102mm wide, 9.5mm thick, 302 stainless steel. The cross-like configuration used is depicted in Figs. 2 and 3. The first rake was located 127mm from the entrance plane of the augmentor tube. The tips of the pitot tubes being 25.4mm from the entrance. The vertical member of this rake was 1.67m high and had seven pitot tubes built into it. Each horizontal member was 0.822m long with three pitot tubes inserted. Horizontal and vertical members were attached as shown in Fig. 4. To hold the rakes in position, 50.8mm high tabs were welded into the augmentor tube at the 12, 3, 6, and 9 o'clock positions. The rakes were then attached to the tabs as shown in Fig. 5. The downstream rake was constructed exactly the same as the first except that the vertical length was 1.70m and each horizontal member was 0.833m long. This second rake was installed 5.05m downstream from the augmentor entrance plane (127mm upstream from the start of the diverging section of the tube). The 6.35mm diameter stainless steel tubing used for the pitot tubes had a wall thickness of 1.57mm. Each tube protruded 101.6mm forward from the rake. The tubes were silver-soldered on the back side of the rake and routed from the augmentor tube at the aft end of each attachment tab through holes drilled in the augmentor.

Tygon tubing (3/16 in. ID x 1/16 in. wall) was then routed from pitot tube to a Scanivalve located in a standing cabinet next to the jet-engine test stand. The output of the Scanivalve was routed through the floor of the cabinet and underneath the test platform to the recording apparatus in the control room (Fig. 6). In addition to the pitot tubes, thermocouples were mounted on each rake as shown in Fig. 2. The thermocouple wire was routed from the augmentor with the pitot tubing, then to ice bath references. The thermocouple data were obtained from a digital voltmeter.

Static pressure ports were located at the 2, 5, 7, and 10 o'clock positions at axial locations 0.152m, 0.305m, 0.610m, 1.212m, 3.96m, 5.18m, 6.10m, and 7.32m downstream of the augmentor inlet. Circumferential ports were used to determine whether or not the flow was axisymmetric. Tygon tubing was attached to Swagelock fittings at each port and routed to a second Scanivalve in the standing cabinet.

In order to determine the velocity of the secondary (test cell) air, velocimeters were located 0.6m and 1.8m above the TF34 engine. The velocimeters used were Datametrics Air Flow Meters, commonly used to measure the velocity in air conditioning ducts. Prior to their use, calibration was performed at the NPS using a small wind tunnel. The resulting calibration curve is shown in Fig. 7. The output of these velocimeters were routed underneath the jet engine test stand to the standing cabinet and then to the control room as described above. In the control room the output signals were connected to a digital voltmeter.

The instrumentation apparatus set up in the control room (Fig. 6) consisted of a locally manufactured Scanivalve controller, two Doric

digial voltmeters and two Honeywell "Electronic 196", 2 pen strip chart recorders.

D. EXPERIMENTAL PROCEDURE

Prior to actual data acquisition the following steps were performed:

1) The 30.5 cm radial gap between the second and third augmentor sections was blocked off with 1.9 cm thick plywood. This was done to prevent any secondary cell air from entering the augmentor downstream of the data acquisition equipment. It should be noted that an airtight seal was not attempted.
2) All static and dynamic pressure ports were pressure checked to insure proper connections and identification.
3) All thermocouples were checked for proper rake attachment, wiring and identification.

The actual data acquisition process began before anticipated due to inadequate thermocouple installation. After initial TF34 start up and a brief run time (during which the recording instruments were calibrated) the test cell operators discovered an oil leak in the TF-34 and consequently shut it down for repair. This provided an opportunity to inspect the test equipment. At this time it was discovered that the thermocouples were not suitably constructed to withstand a complete series of tests. Therefore, it was decided to record termperature data during the initial TF-34 bearing breakin tests at various power settings for as long as the thermocouples remained in place. Reliable temperature data were only obtained for maximum, 90%, and idle power settings. The data appears in Table I.

POWER SETTING	CORE RPM	FAN RPM	THRUST LBS	RAKE	THERMOCOUPLE	TEMPERATURE (°C)
100%	17228	6667	8611	FORWARD	CENTER	438
					LOWER	39
				AFT	CENTER	127
					LOWER	76
90%	16120	5803	5967	FORWARD	CENTER	461
					LOWER	32
				AFT	CENTER	156
					LOWER	62
IDLE	11350	1685	382	FORWARD	CENTER	498
					LOWER	18
				AFT	CENTER	105
					LOWER	42

TABLE I: Thermocouple Data Obtained During Initial Engine Testing

After the brief bearing breakin tests the TF-34 was put through a series of five minute duration tests at a variety of power settings. When a particular power setting was reached two minutes were allowed to insure steady-state operation and then the following data were recorded:

1) From the test cell instrumentation:
    a) ambient temperature
    b) ambient pressure
    c) cell pressure
    d) TF-34 core RPM
    e) TF-34 fan RPM
    f) TF-34 thrust
2) From NPS installed equipment and instrumentation:
    a) static pressures along the augmentor wall
    b) pitot tube pressures at each rake
    c) temperatures at each rake

Each 48 channel Scanivalve was set up so that port number one was open to the cell pressure. A fixed pressure (set using a mercury manometer) was input to port number two in order to provide a reference calibration each time a cycle was begun. During each run one Scanivalve was cycled using the Scanivalve controller, data recorded on the strip chart, connections switched, and the same procedure followed for the remaining Scanivalve. The pitot rakes were labeled as shown in Fig. 8, and static ports as in Fig. 9. The recorded data are presented in Tables II through IV, the letter "A" referring to the forward rake, "B" to the aft rake, and letters "C through J" to the

static port stations from front to rear. The data obtained from the intermediate power setting run was not utilized due to lack of reliable temperature information at that thrust level.

There were three specific problems encountered during the data acquisition process:

1) Failure of thermocouple attachments. This resulted in lack of temperature data during each run that pressure data were obtained. However, this was overcome by correlating (by thrust setting and fan and core speeds) the temperature data recorded at the start of the TF-34 test series with the pressure data obtained later.

2) During the entire test series a loud resonant frequency was heard. This initially forced engine shut down to allow for cell inspection. No damage was discovered and all instrumentation appeared normal so testing was continued as planned. However, upon removal of test equipment it was discovered that two of the welds holding the aft rake in place had broken. It should also be noted that at the same time it was discovered that two pitot tubes had detached from the same rake. The latter apparently occurred during the last test since no unusual change occurred in the recorded data.

3) Due to electrical connection difficulties the velocimeters were not installed during the engine testing periods when other data were obtained. When this problem was corrected (after the pressure data were obtained) it was discovered that the wooden blocks

RUN NO.: 1 POWER SETTING: 100% TIME: 1305

PITOT RAKE ($p-p_{CELL}$)			STATIC PORT ($p-p_{CELL}$)		
SCANIVALVE CHANNEL	PORT I.D.	($N/m^2 x10^{-3}$)	SCANIVALVE CHANNEL	PORT I.D.	($N/m^2 x10^{-3}$)
1	Zero		1	Zero	
2	REF PRES		2	REF PRES	
3	A1	34.30	3	C1	-14.196
4	A2	39.93	4	C2	-13.776
5	A3	3.56	5	C3	-13.803
6	A4	-0.63	6	C4	-14.266
7	A5	41.11	7	D1	-13.218
8	A6	5.97	8	D2	-12.797
9	A7	-0.48	9	D3	-12.956
10	A8	39.58	10	D4	-13.190
11	A9	3.78	11	E1	-9.694
12	A10	-0.84	12	E2	-9.370
13	A11	40.19	13	E3	-9.432
14	A12	2.68	14	E4	-9.860
15	A13	-0.48	15	F1	-8.226
16	B1	26.84	16	F2	-8.226
17	B2	19.81	17	F3	-8.226
18	B3	8.39	18	F4	-8.226
19	B4	3.30	19	G1	-6.433
20	B5	23.24	20	G2	-6.661
21	B6	10.36	21	G3	-6.530
22	B7	3.12	22	G4	-6.433
23	B8	18.71	23	H1	-6.268
24	B9	7.51	24	H2	-6.171
25	B10	1.28	25	H3	-5.875
26	B11	15.59	26	H4	-6.33
27	B12	5.76	27	I1	-4.144
28	B13	0.04	28	I2	-4.013
			29	I3	-3.820
			30	I4	-4.047
			31	J1	-1.731
			32	J2	-1.958
			33	J3	-2.027
			34	J4	-1.827

	FAN	CORE
RPM:	6701	17360

THRUST: 8685 (LBS)

	CELL	RAKE A	RAKE B
TEMP: (°C)	17.8		

	CELL	AMBIENT
PRESSURE: (N/m^2)	$1.0129 x10^5$	$1.0141 x10^5$

TABLE II: EXPERIMENTAL DATA, 100% POWER

RUN NO: 3 POWER SETTING: 90% TIME: 1327

PITOT RAKE ($p-p_{CELL}$)			STATIC PORT ($p-p_{CELL}$)		
SCANIVALVE CHANNEL	PORT I.D.	($N/m^2 x10^{-3}$)	SCANIVALVE CHANNEL	PORT I.D.	($N/m^2 x10^{-3}$)
1	Zero		1	Zero	
2	REF PRES		2	REF PRES	
3	A1	22.64	3	C1	-9.29
4	A2	30.86	4	C2	-10.08
5	A3	0.49	5	C3	-9.56
6	A4	-0.39	6	C4	-9.29
7	A5	29.04	7	D1	-9.23
8	A6	4.18	8	D2	-9.23
9	A7	-0.19	9	D3	-9.33
10	A8	30.60	10	D4	-9.45
11	A9	2.58	11	E1	-7.46
12	A10	-0.29	12	E2	-6.70
13	A11	31.71	13	E3	-7.07
14	A12	3.65	14	E4	-7.55
15	A13	-0.26	15	F1	-5.71
16	B1	20.64	16	F2	-5.62
17	B2	16.86	17	F3	-5.53
18	B3	8.18	18	F4	-5.59
19	B4	1.60	19	G1	-4.14
20	B5	17.30	20	G2	-4.41
21	B6	8.41	21	G3	-4.41
22	B7	3.16	22	G4	-4.26
23	B8	13.96	23	H1	-4.08
24	B9	5.83	24	H2	-3.87
25	B10	1.38	25	H3	-3.75
26	B11	12.72	26	H4	-4.12
27	B12	3.96	27	I1	-2.76
28	B13	0.98	28	I2	-2.79
			29	I3	-2.45
			30	I4	-2.61
			31	J1	-1.10
			32	J2	-1.40
			33	J3	-1.40
			34	J4	-1.34

	FAN	CORE
RPM:	5933	16403

THRUST: 6304 (LBS)

	CELL	RAKE A	RAKE B
TEMP: (°C)	18.3		

	CELL	AMBIENT
PRESSURE: (N/m^2)	$1.0136 x10^5$	$1.0144 x10^5$

TABLE III: EXPERIMENTAL DATA, 90% POWER

RUN NO: 4 POWER SETTING: IDLE TIME: 1337

PITOT RAKE ($p-p_{CELL}$)			STATIC PORT ($p-p_{CELL}$)		
SCANIVALVE CHANNEL	PORT I.D.	($N/m^2 x10^{-3}$)	SCANIVALVE CHANNEL	PORT I.D.	($N/m^2 x10^{-3}$)
1	Zero		1	Zero	
2	REF PRES		2	REF PRES	
3	A1	1.44	3	C1	-0.64
4	A2	2.56	4	C2	-0.77
5	A3	0.45	5	C3	-0.74
6	A4	0.27	6	C4	-0.71
7	A5	2.52	7	D1	-0.71
8	A6	0.41	8	D2	-0.74
9	A7	0.27	9	D3	-0.74
10	A8	2.43	10	D4	-0.71
11	A9	0.27	11	E1	-0.58
12	A10	0.14	12	E2	-0.49
13	A11	2.48	13	E3	-0.52
14	A12	0.23	14	E4	-0.55
15	A13	0.14	15	F1	-0.40
16	B1	1.53	16	F2	-0.43
17	B2	1.48	17	F3	-0.40
18	B3	0.54	18	F4	-0.43
19	B4	0.50	19	G1	-0.28
20	B5	0.27	20	G2	-0.28
21	B6	1.35	21	G3	-0.25
22	B7	1.35	22	G4	-0.28
23	B8	0.36	23	H1	-0.28
24	B9	1.12	24	H2	-0.18
25	B10	0.54	25	H3	-0.18
26	B11	0.32	26	H4	-0.15
27	B12	1.12	27	I1	-0.03
28	B13	0.41	28	I2	-0.03
			29	I3	0
			30	I4	0
			31	J1	-0.03
			32	J2	0
			33	J3	0
			34	J4	0

	FAN	CORE
RPM:	1801	11404

THRUST: 410 (LBS)

	CELL	RAKE A	RAKE B
TEMP: (°C)	18.3		

	CELL	AMBIENT
PRESSURE: (N/m^2)	$1.0144 x10^5$	$1.0144 x10^5$

TABLE IV: EXPERIMENTAL DATA, IDLE POWER

at the intersection of the second and third augmentor sections had partially detached. This caused the velocity of the cell air to probably be somewhat higher during the tests using the velocimeters than it was during the pressure/acquisition runs when the blocks were in place. The velocimeter data are shown in Table V. These data were used only to obtain the general shape of the velocity profile above the engine.

E. DATA REDUCTION

The $(p-p_{cell})$ data that appear in Tables II through IV came directly from the strip chart recordings, or, in the case where the reading was too small, from the digital voltmeter. The calibration scale on the strip chart (psi/division) was obtained from a 1.05 in. Hg reference input to Channel No. 2 of both Scanivalves. Using this information, axial pressure profiles along the four circumferential positions were plotted and an average pressure profile was then estimated for each power setting (Figs. 10, 11, and 12). These profiles were then used to obtain the static pressure at the aft rake location (it was assumed that pressure was uniform across the augmentor at the aft rake).

The measured stagnation pressure at each pitot tube together with the static pressure at the rake were used to obtain a Mach number profile using the expression

$$\frac{P_T}{p} = \left[1 + \frac{\gamma - 1}{2} M^2\right]^{\frac{\gamma}{\gamma - 1}}$$

Velocity (m/sec)		RPM		Thrust (lbs)
Upper Velocimeter	Lower Velocimeter	Fan	Core	
0.51	1.14	1789	11265	520
2.03	3.05	6780	17285	9072

TABLE V: VELOCIMETER DATA

with γ assumed equal to 1.4. The thermocouple readings were plotted and used to estimate an assumed axisymmetric stagnation temperature profile for the aft rake at each power setting (Fig. 13). The estimated stagnation temperature profile and local Mach number were then used to determine a static temperature for each pitot tube location. Using this information and the properties of air at standard temperature and pressure, accoustic speed and velocity were found for each pitot tube position. Static temperature for the aft rake is plotted as a function of radius in Fig. 14, velocity profiles are shown in Figs. 15, 16, and 17.

The static pressure of the front rake was estimated by extrapolating the average pressure profile to the augmentor inlet position. This was required due to the fact that the first set of static pressure ports was installed 15.2 cm aft of the augmentor entrance plane. This static pressure was assumed to be uniform across the augmentor for each power setting. Mach number profiles were then obtained as above. At the forward rake γ was not assumed to be uniform across the augmentor. Instead, γ was taken to be 1.33 at the centerline position and at the four pitot tubes located circumferentially 25.4 cm from the center. At the remaining positions γ was assumed to be 1.4. This property change was made since heat induced discoloration on the forward rake was observed to occur from the core jet to a radius of approximately 30 cm. Stagnation temperature profiles were estimated using the measured temperatures at the two rake locations and are shown in Fig. 18. Using this stagnation temperature distribution with the Mach number profiles, accoustic

speed and velocity were determined as above. The resulting velocity profiles for each power setting are shown in Figs. 19 through 21.

III. COMPUTER MODEL

A. INTRODUCTION

The computer program used to model the turbojet test cell of this investigation was the CHAMPION/2/E/FIX computer program developed by Pun and Spalding [Ref. 7] was modified by Stevenson [Ref. 1]. This is a primitive variable (pressure-velocity) model for two-dimensional, turbulent recirculating flows. The equations are cast into finite difference form and solved using a line-by-line iteration method. A detailed discussion of the model can be found in Refs. 1 and 7.

B. PHYSICAL MODEL

The major modifications made to the computer program as utilized by Stevenson [Ref. 1] were to change the geometry of the test cell and to incorporate the engine exhaust velocity profile of the TF-34 turbofan engine.

The turbojet test cell, TF-34 engine and augmentor dimensions used in the computer model are shown in Fig. 22. There were several differences between the configuration used in the computer model and the actual test cell as shown in Fig. 22:

1. The computer model was axisymmetric and therefore required the engine to be located on the axis of symmetry of the test cell. In the actual cell the engine is approximately 0.61m closer to the deck than to the overhead. Thus, it can be expected that the predicted velocity distribution of the secondary cell air would be somewhat different than the actual distribution. In addition,

the test stand and supporting deck probably distorted the velocity profile at the augmentor inlet.

2. The exhaust of the TF-34 turbofan engine was modeled as two concentric cylinders (gas generator core and fan exhausts). In reality, each exit incorporates a converging nozzle. For simplicity in the two-dimensional model, the actual exit diameter of each duct was utilized over the entire engine length (Figs. 23 and 24).
3. In the computer model the aft cell wall was taken to coincide with the augmentor inlet. This wall was actually approximately 11m farther back. The effect of this modification was to eliminate the recirculation zone above the augmentor tube. However, the effects of this low velocity recirculation zone above the augmentor flow field have been shown to be insignificant [Ref. 5].
4. The computer model utilized a constant diameter augmentor tube 20.5m long instead of the varying area tube construction shown in Fig. 1. The second rake was not positioned farther downstream to avoid complications arising from the divergent character of the second augmentor section and the flow disturbance expected to result from the water injection ring and noise suppression devices. The augmentor tube length was modelled as 20.5m versus the actual 5.05m so that the boundary conditions at the exit plane would not influence the calculations at the position of the second rake.
5. The test cell was square in cross-section. This was modelled as a concentric cylinder with the same cross-sectional area.

The grid spacing for the finite difference numerical solution of this problem was crucial. A 30 by 30 grid was used originally without obtaining convergence. Consequently the grid was expanded to a 40 by 30 to better accommodate the much greater length of the axial direction. The recommendation by Gosman et al [Ref. 3] that successive spacing should not increase by more than a factor of approximately 1.5 was adhered to.

C. DATA INPUT

Using the empirical velocity profiles from Figs. 15 through 17, an average velocity for each radial position at the aft rake was determined. These average velocities and the centerline velocity were then plotted (Fig. 25) and graphically integrated to obtain a one-dimensional bulk velocity at the aft rake for each power setting. An identical procedure was followed to obtain an average static temperature (Fig. 14) at the aft rake. These results were then used (together with the standard properties of air and known augmentor tube cross sectional area) to calculate the total mass flow rate through the augmentor tube.

Using the fan and core RPM, thrust, and engine inlet temperatures that appear in Tables II through IV, fan and core mass flow rates for the TF-34 were obtained from the General Electric Corp., Lynn, Mass. It should be noted that the flow rates provided by General Electric were for "an ideal" engine and may not exactly apply to the specific engine used in this investigation.

With the above flow rates it was then possible to calculate the mass flow rate through the test cell. Then, using the temperature and pressure in the test cell (and the known cell cross sectional area) the average one-dimensional velocity of the cell air was determined.

In this investigation no instrumentation was available for measuring static pressures and temperatures at the TF-34 core and fan tailpipe exhausts. Turbine exit temperature as a function of thrust is presented in Ref. 8.

This temperature was used as the tailpipe stagnation temperature in order to calculate nozzle exhaust temperature. For the idle power setting the Mach number at the core exit was assumed to be approximately 0.5 and γ to be 1.33. Using a turbine exhaust temperature of 1560°R resulted in a nozzle discharge static temperature of 1498°R. For the 90% and full power cases the nozzle flow was choked and the turbine exhaust temperatures were 1694°R and 1922°R respectively. This resulted in exhaust temperatures of 1453°R and 1649°R respectively. Fan exhaust temperatures were available from the temperature profiles of Ref. 8. Actual cross sectional areas of both exhaust nozzles were measured on the engine. Static pressure at the exhaust nozzles was taken to be the static pressure of the cell in all cases. This static pressure estimate is accurate for the fan exhaust in all cases and the core exhaust at the idle power setting. However, the static pressure of the core exhaust for the maximum and 90% power settings was actually the critical pressure.

Using the above information the one-dimensional continuity equation was used to calculate the bulk velocities for core and fan exhausts at all power settings. The computer input data as well as the CPU time required to obtain a converged solution for each power setting are shown in Table VI.

POWER SETTING		TEMPERATURE (°K)	VELOCITY (m/sec)	CELL-PRESSURE ($N/m^2 x 10^{-3}$)	CPU TIME (IBM 360/67) (min)
	CELL	291	0.825	101.5	75
IDLE	FAN	344	56.04		
	CORE	832	59.63		
	CELL	291	2.75	101.37	75
90%	FAN	305	174.2		
	CORE	807	258.8		
	CELL	290	3.52	101.30	150
100%	FAN	306	202.9		
	CORE	916	354.1		

TABLE VI. COMPUTER INPUT DATA

IV. DISCUSSION OF RESULTS

A. INTRODUCTION

The results of this investigation are presented in the following manner:

1) General characteristics and accuracy of the experimental data and sensitivity of the calculated experimental velocity profiles to assumptions made for the unknown/unmeasured experimental parameters.

2) A comparison of experimental data to computer model predictions and the sensitivity of the predictions to uncertainties in the data.

B. EXPERIMENTAL DATA

Experimental data are presented in Tables II through IV. The resulting calculated velocity profiles for the fore and aft rakes at each power setting are presented in Figs. 19 through 21 and Figs. 15 through 17, respectively. Figs. 10 through 12 show the static pressure profiles along the augmentor wall for each power setting.

The pressure profiles show only a small variation with circumferential location. In all cases the minimum pressure occurred very close to the inlet plane of the augmentor, whereas the maximum pressure in the instrumented portion of the augmentor at no time exceeded atmospheric. As expected, the minimum pressure at the augmentor inlet decreased as the engine flow rate increased, going from -0.8×10^{-3} N/m^2 at the idle power setting to -14.0×10^{-3} N/m^2 at the maximum power condition.

The velocity profiles at the aft rake indicate that the flow was not axisymmetric in the augmentor tube. The most asymmetric condition occurred at the idle power setting. The idle profile was also much more fully developed than the others, indicating that the flow at idle was the only one that entered the diverging section of the augmentor tube in a reasonably well mixed condition. There also appeared to be a general trend toward higher mass flow in the quadrant defined by the 12 and 3 o'clock positions.

In all cases the velocity profiles at the forward rake showed the expected high velocity near the center with the lower fan and augmentor air velocities toward the wall. It should also be noted that the spread in data at the forward rake was much less than that at the aft rake.

In all cases the engine-exit-to-augmentor-inlet spacing was 1.7m. At the idle power setting the augmentation ratio was 2.39:1. This ratio dropped to 2.22:1 for the 90% power case and rose to 2.42:1 for the maximum power setting.

In summary it can be said that the static pressure remained quite uniform across the tube, that the flow at the aft rake was not axisymmetric, and that at the front pitot rake the flow was quite symmetrical.

For the 90% power setting the stagnation pressure data at the aft rake was estimated to have an uncertainty of 0.17% which, in turn, resulted in a 0.25% uncertainty in the calculated velocities. Similarily, the static pressure readings were examined and found to have an uncertainty of approximately 2% near the aft rake. This uncertainty in static pressure resulted in approximately a 5% uncertainty in the velocities at the aft rake.

The possibility that the total temperature profile at the aft rake was not that estimated in Figure 13 was also examined. A somewhat different, but plausible, total temperature profile was plotted and is shown in Fig. 26 for 90% power. This change in the T_T profile resulted in a 4.7% increase in the bulk static temperature and a 1.3% increase in the bulk static temperature and a 1.3% increase in the bulk velocity. These changes would result in a 4.8% decrease in the test cell mass flow rate (assuming engine flow rates were known).

Finally, the assumption that the specific heat ratio was not 1.4 at the aft rake was examined. Changing γ to 1.35 resulted in insignificant changes in the cell flow rate.

The experimental data for the forward rake were also examined to discover how uncertainties in static pressure and stagnation temperature profiles would affect the predicted velocities. Possible errors in the extrapolated pressure at the forward end of the pitot tubes resulted in an uncertainty of only 4.5% (Fig. 27) in the velocities. The velocity profile is sensitive to the assumed stagnation profile in much the same manner as discussed above for the aft rake.

C. COMPUTER MODEL PREDICTIONS

The pressure and velocity profiles that resulted from computer modelling are presented with the actual experimental data for each power setting in Figs. 10 through 12, 15 through 17, and 19 through 21.

Sensitivity of the computer model predictions to specified test cell mass flow rate and engine mass flow rate were examined. A 10% decrease in engine mass flow rate was found to alter the computer model results an insignificant amount. This is attributable to the lesser

contribution of the engine to the total flow rate through the augmentor. A 10% decrease in the specified test cell mass flow rate decreased the predicted velocity at the front rake a maximum of 10%. The maximum decrease occurred near the augmentor wall, where the cell flow rate had the greatest influence. At the aft rake the 10% decrease in specified cell flow rate caused a maximum decrease in velocity of 7%, again near the augmentor wall. This decrease in specified flow rate caused the static pressure drop to decrease approximately 20%. These results are shown for the 90% power case in Figs. 28 and 29.

The theoretical velocity profiles at the forward rake appear to be in good agreement with the experimental results. However, the experimental results showed less variations near the centerline than predicted. The predictions underestimated the centerline velocities at idle and 90% power and overestimated it at 100% power.

The experimentally obtained aft rake velocities at idle power had considerable circumferential variations. The theoretical predictions, which are based on axisymmetric flow, appeared to be a reasonable estimation of the average behavior. In both the 90% and maximum power cases the computer model predicted a good velocity profile although the velocities were considerably greater (up to 63%) than the experimental values. This occurred to a greater extent at maximum power, indicating a possible decrease in predictive accuracy as mass flow rate was increased. Inaccurate specification of engine flow rates can significantly alter the cell flow rate input to the computer model. This in turn can significantly affect the predicted velocity profiles as discussed above. Inaccurate stagnation profiles can also contribute to errors in model

input data as discussed above. However, these possible inaccuracies cannot account for the entire difference in results obtained at full power.

The theoretical pressure profiles (Figs. 10, 11, and 12) in all three cases indicate a large pressure drop at the augmentor tube inlet plane. The pressure decrease was greater at the augmentor wall than along the engine centerline . This theoretical drop in pressure was greater than the experimental pressure drop, the difference increasing with an increase in mass flow rate. The pressure rise from the minimum was in better agreement with the data but also was less accurate at higher power settings. The predicted behavior being much greater than experimental results is similar to the results of Walters and Netzer [Ref. 6] using the ψ-ω computer code and to the results of Stevenson and Netzer [Ref. 1] using the primitive variable code. In these earlier studies which compared predictions to experimental data in a one eighth scale test cell, good agreement in pressure profiles was obtained for zero engine-augmentor spacing. The discrepancy increased with increasing engine-augmentor spacing. One possible cause of this disagreement is the K-ε turbulence model. It is being used in this application for the shear layer mixing of a practically unconfined jet surrounded by a very low velocity flow, both of which must then enter a confined diameter.

Sensitivity of the computer model predictions to the magnitude of the effective viscosity was examined in a cursory manner by both increasing and decreasing the calculated values by a factor of 1.5. The computer model predictions were found to be fairly insensitive to these changes in calculated effective viscosity. For the case of a 50% increase in viscosity

Figs. 30 and 31 show less than 5% change in velocity at the front rake, 15% at the aft rake, and no greater than a 6% decrease in static pressure drop along the augmentor wall. A 33% decrease in viscosity changed velocity at the front rake less than 5%, 10% at the aft rake and decreased the static pressure drop along the augmentor wall no more than 9% (Figs. 32 and 33). It appears that merely changing the magnitude of the effective viscosity will not account for the differences in the predicted and measured pressure profiles. Further investigations of the two-parameter effective viscosity model are required.

The sensitivity of the static pressure profiles to possible inaccuracies in model inputs can account for much of the discrepancies at idle power but not for 90% and full power.

Thus, it appears from both the velocity and pressure profile data that the predictive accuracy of the model decreases with increasing engine exit Mach number.

Examination of the data from the velocimeters positioned above the TF-34 showed a test cell air velocity profile which increased from ceiling to engine. However, it has been shown by Speakman, Hayes, and Netzer [Ref. 5] that this condition has an insignificant effect on the predicted velocity and pressure profiles in the augmentor.

The computer model appears to have the same capabilities and weaknesses in predicting the flow in full scale test cells as it did for the subscale test cell. The subscale test cell, by design, provided nearly axisymmetric flow in the augmentor at all power settings and therefore somewhat better agreement was obtained for predicted velocity profiles far down the augmentor tube. Engine flow rates were also more

accurately known in the subscale tests. The most severe weakness of the model appears to be in the inability to correctly predict accurate static pressure profiles in regions where an expanding high velocity jet is captured by a fixed diameter tube. Velocity profiles and mixing rates appear to be reasonably predicted.

V. CONCLUSIONS AND RECOMMENDATIONS

The two-dimensional, primitive-variable computer model proved to be quite good in predicting velocity profiles and mixing rates in the augmentor tube of a full scale jet engine test cell. The major weakness in this area was that the magnitude of the velocities far downstream were somewhat higher than actual with the discrepancy increasing with increasing engine exhaust Mach number (i.e. power setting).

The greatest drawback to the computer model was its inability to accurately predict static pressure profiles in the augmentor entrance region where an expanding high velocity jet is captured by a fixed diameter tube. This inaccuracy also was found to increase with engine power level.

If time and cost pose less restraints to future investigators it is recommended that the data gathering apparatus be expanded to include pitot-static and temperature measuring equipment at all locations where velocity data are desired. This would preclude the necessity for making the assumptions required in this investigation for stagnation temperature profiles.

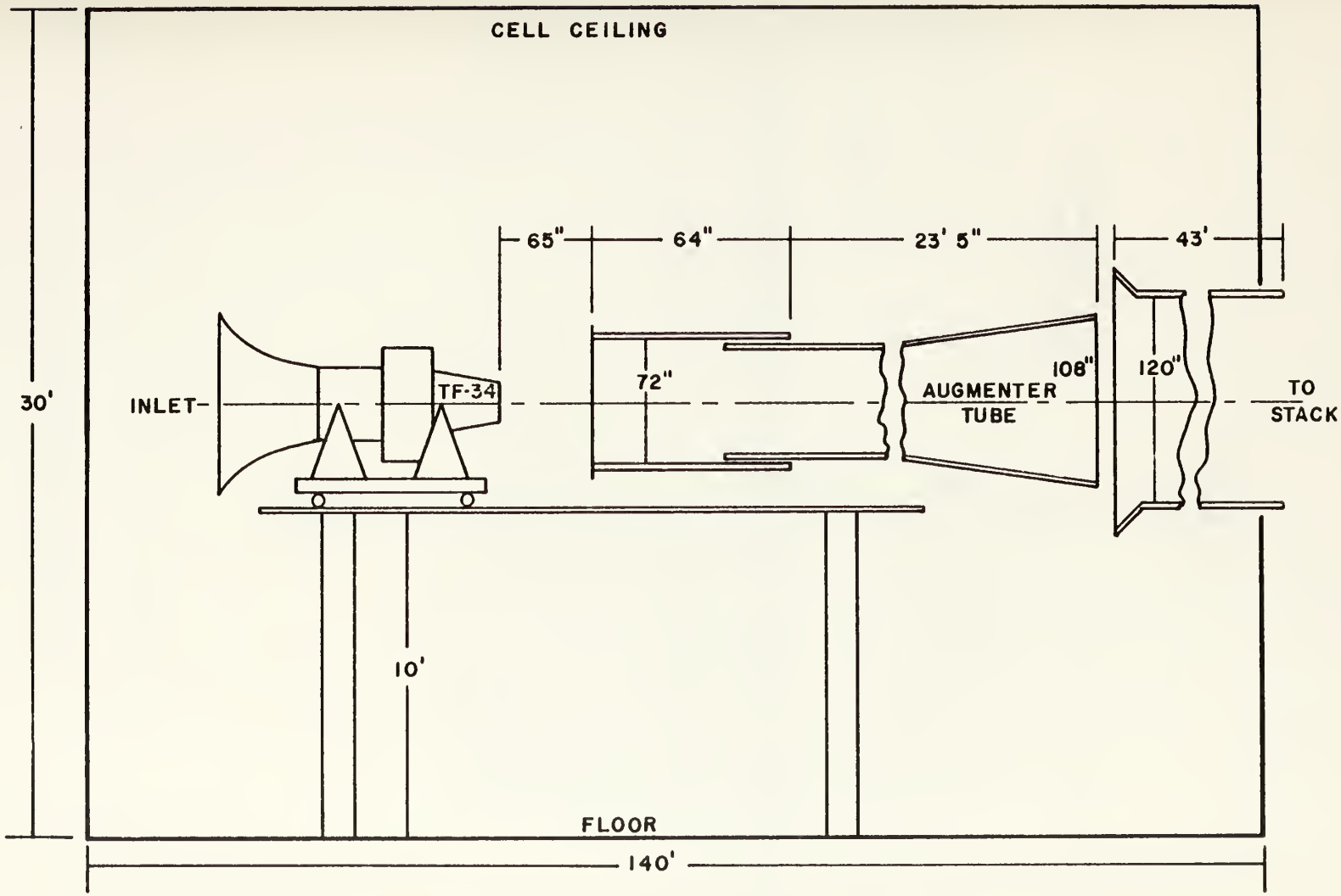

Fig. 1 TF-34 Test Configurations

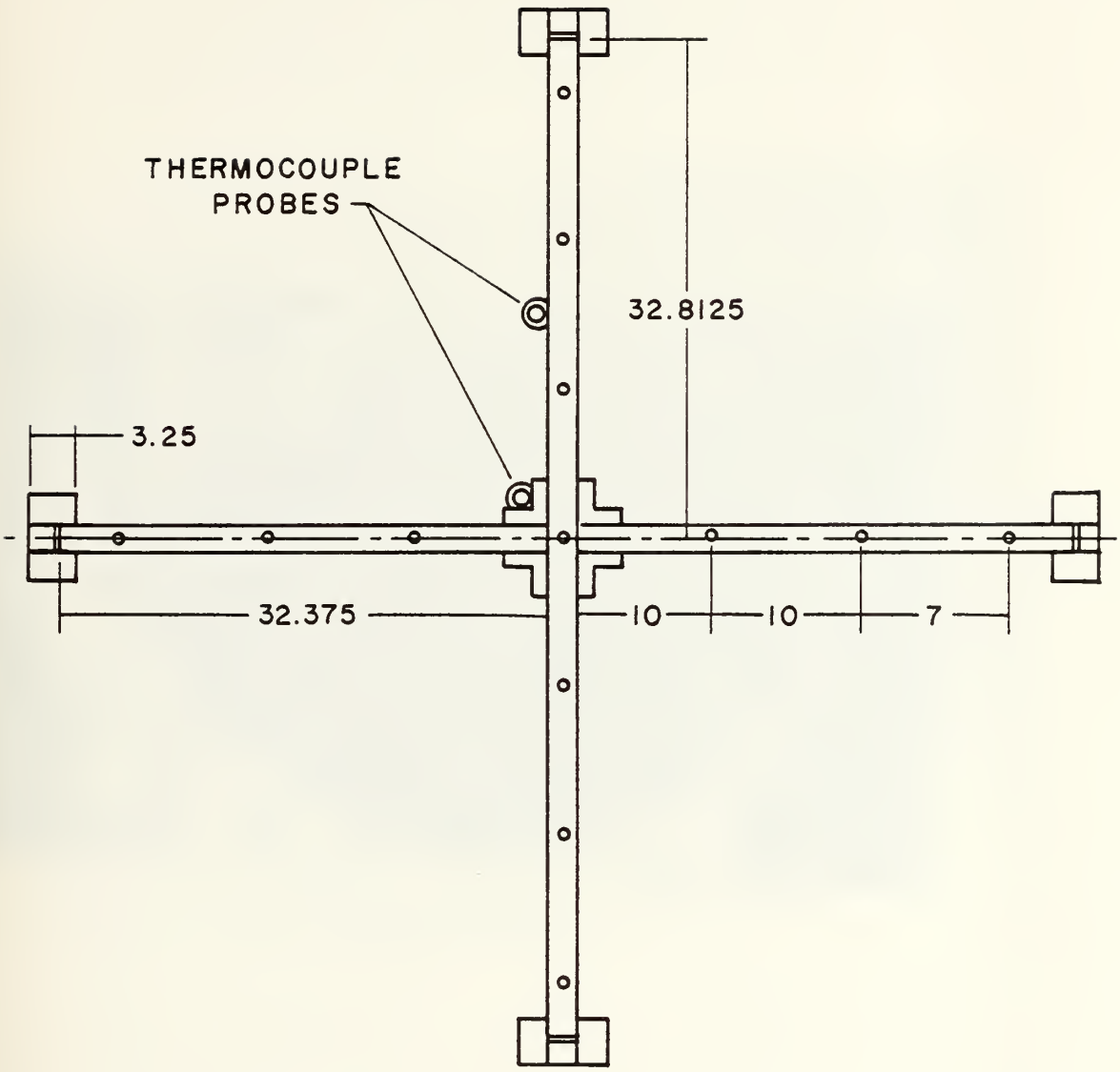

Fig. 2 Pitot Rake Front View

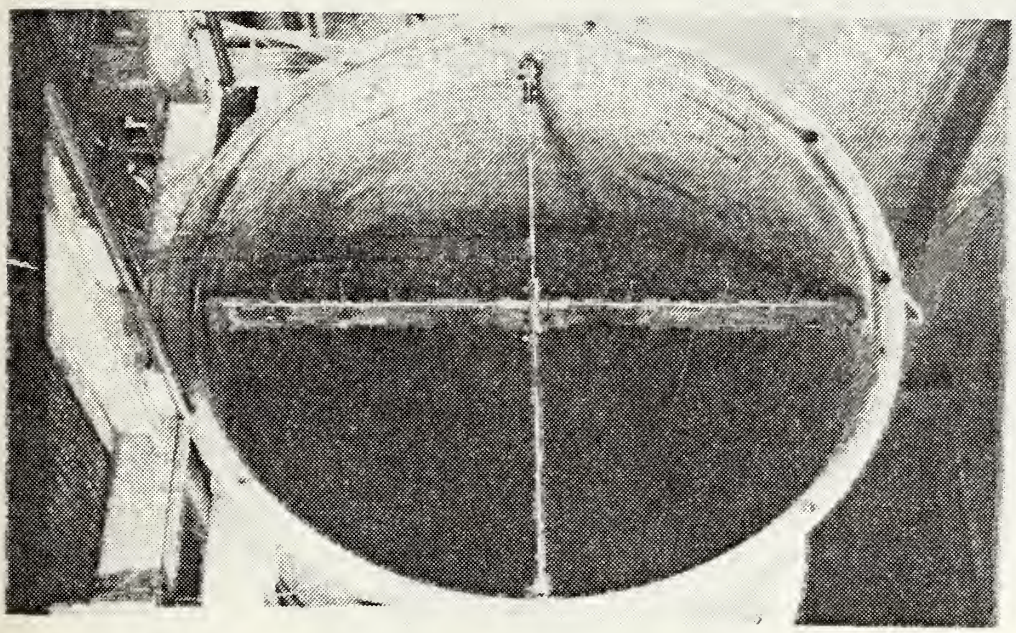

Fig. 3 Pitot Rake Mounted in Augmentor Tube

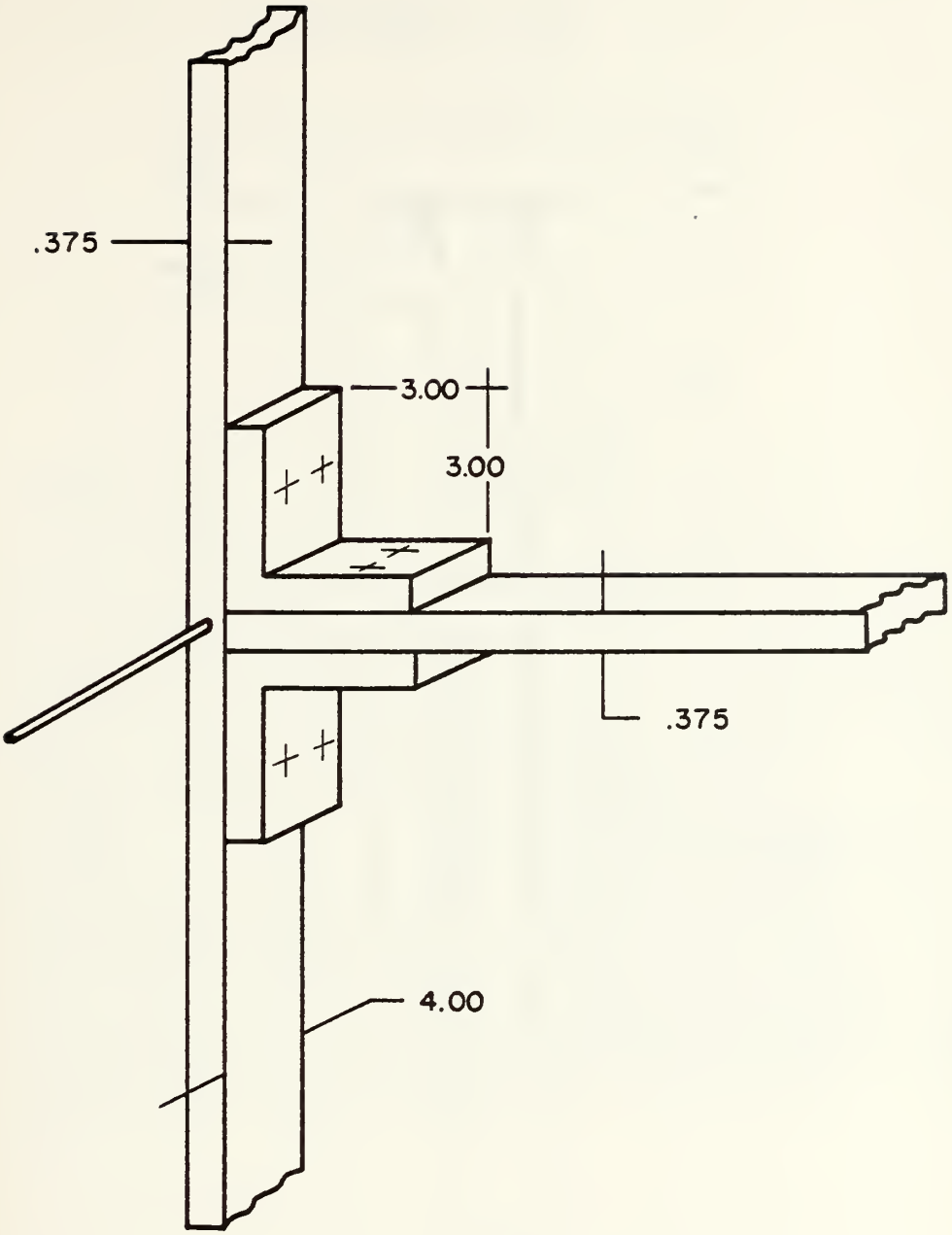

Fig. 4 Pitot Rake Contruction

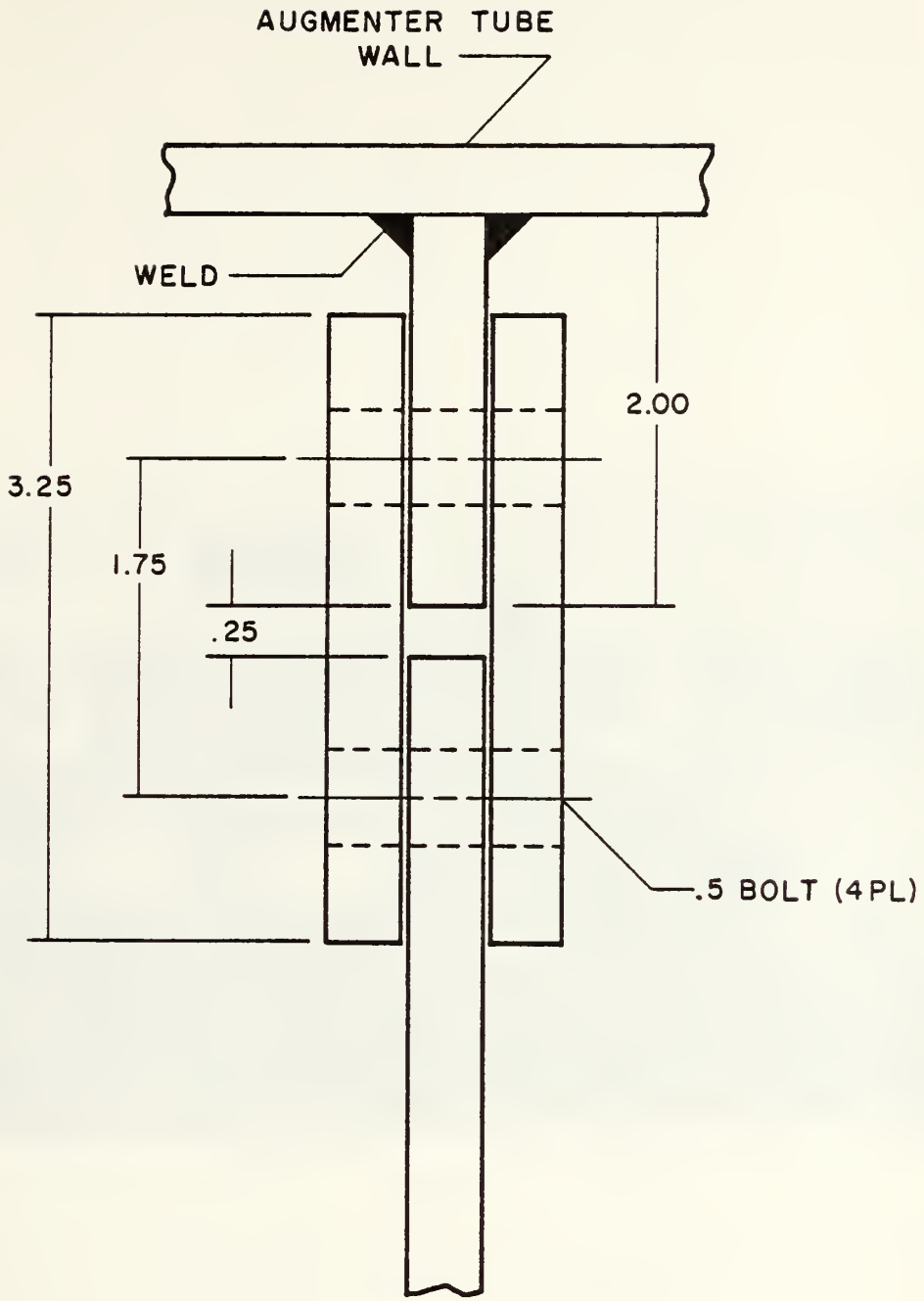

Fig. 5 Rake Attachment

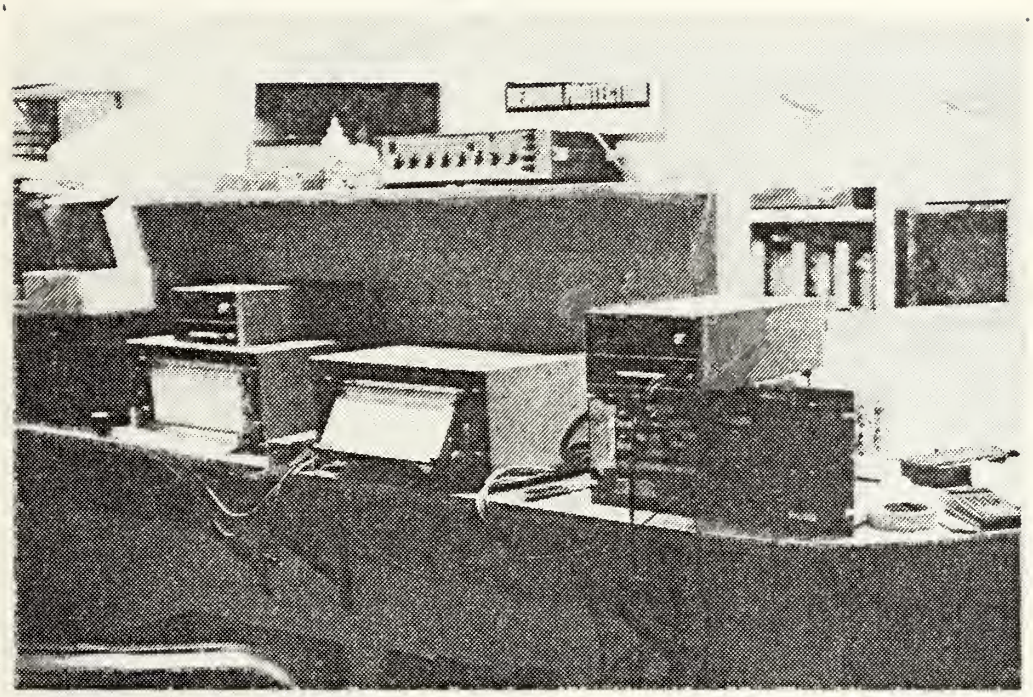

Fig. 6 Instrumentation

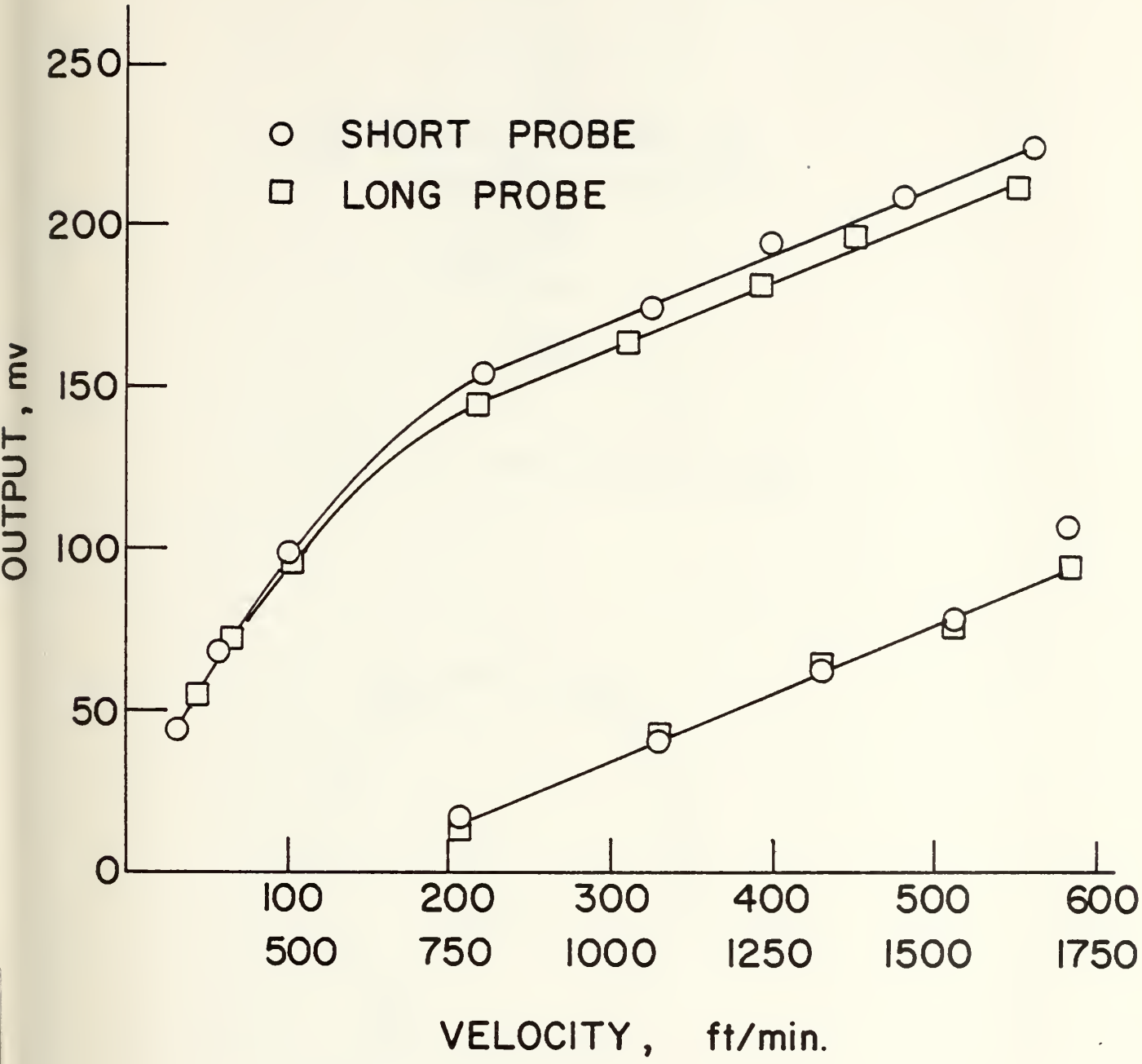

Fig. 7 Velocimeter Calibration Curves

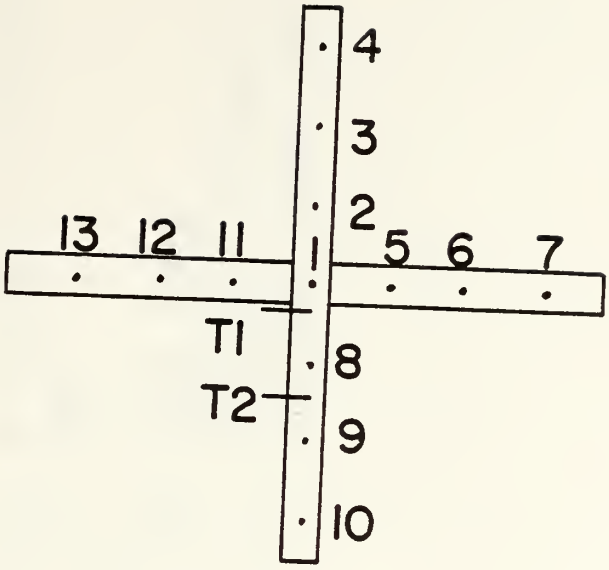

Fig. 8 Pitot Tube/Thermocouple Labels

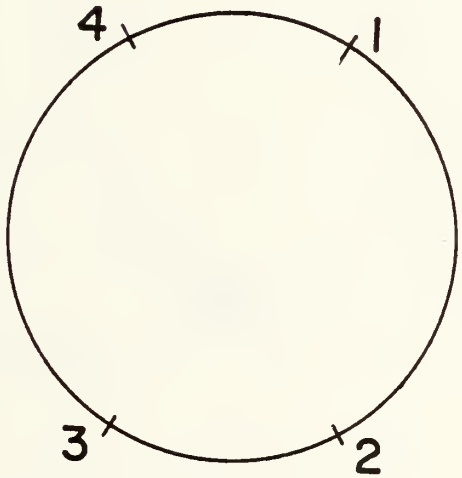

Fig. 9 Static Port Labels

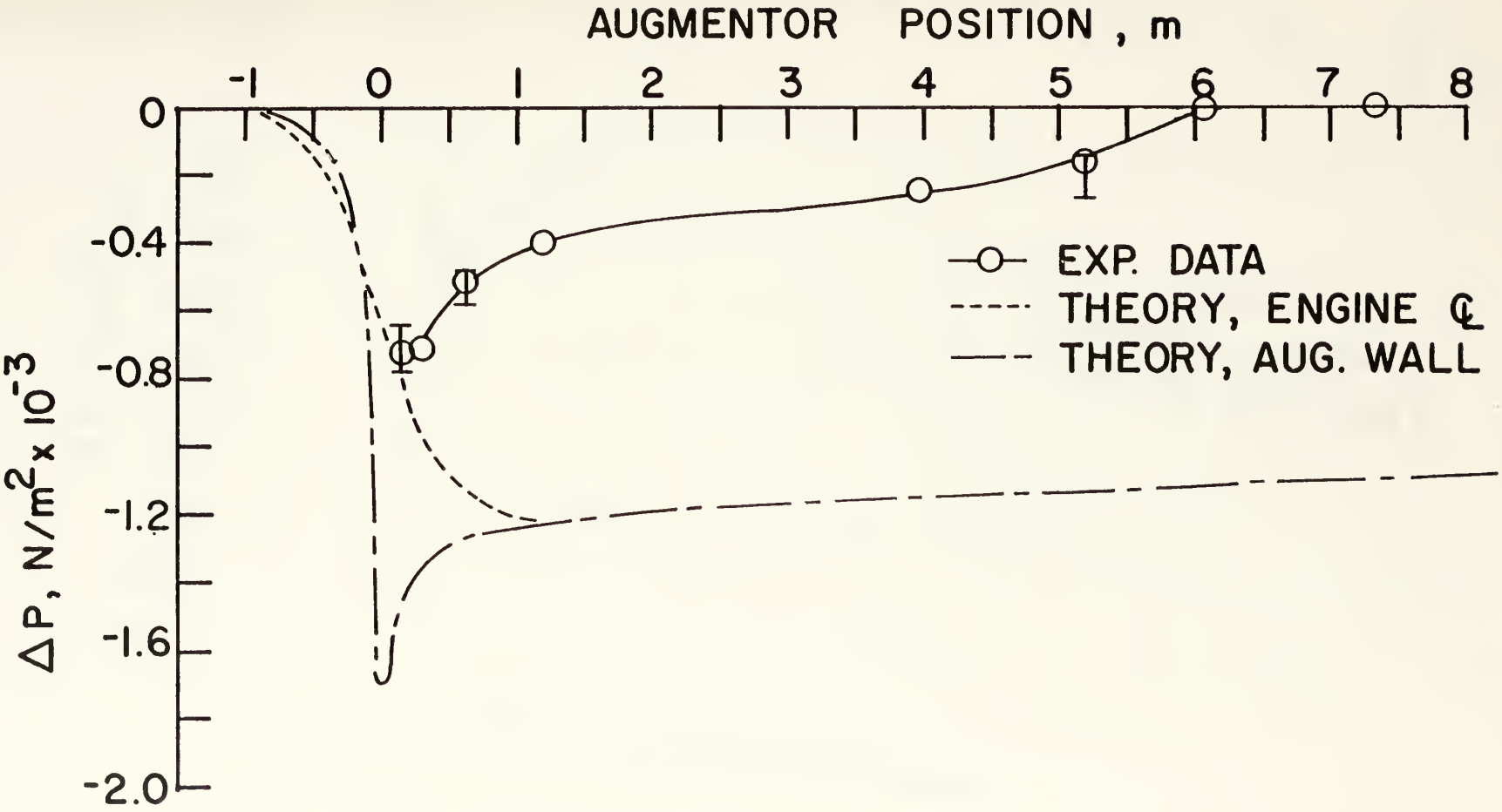

Fig. 10 Pressure Profile, Idle Power

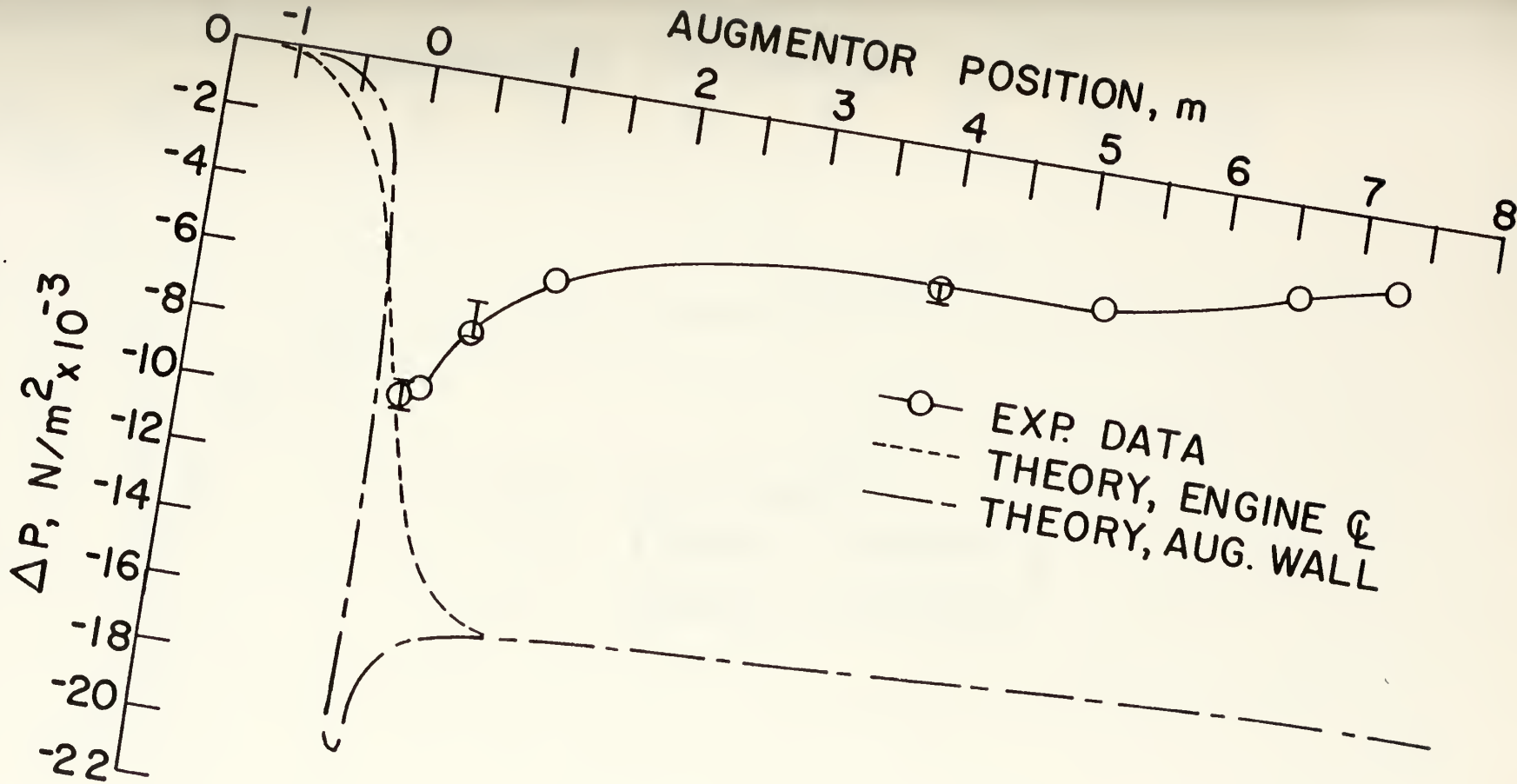

Fig. 11 Pressure Profile, 90% Power

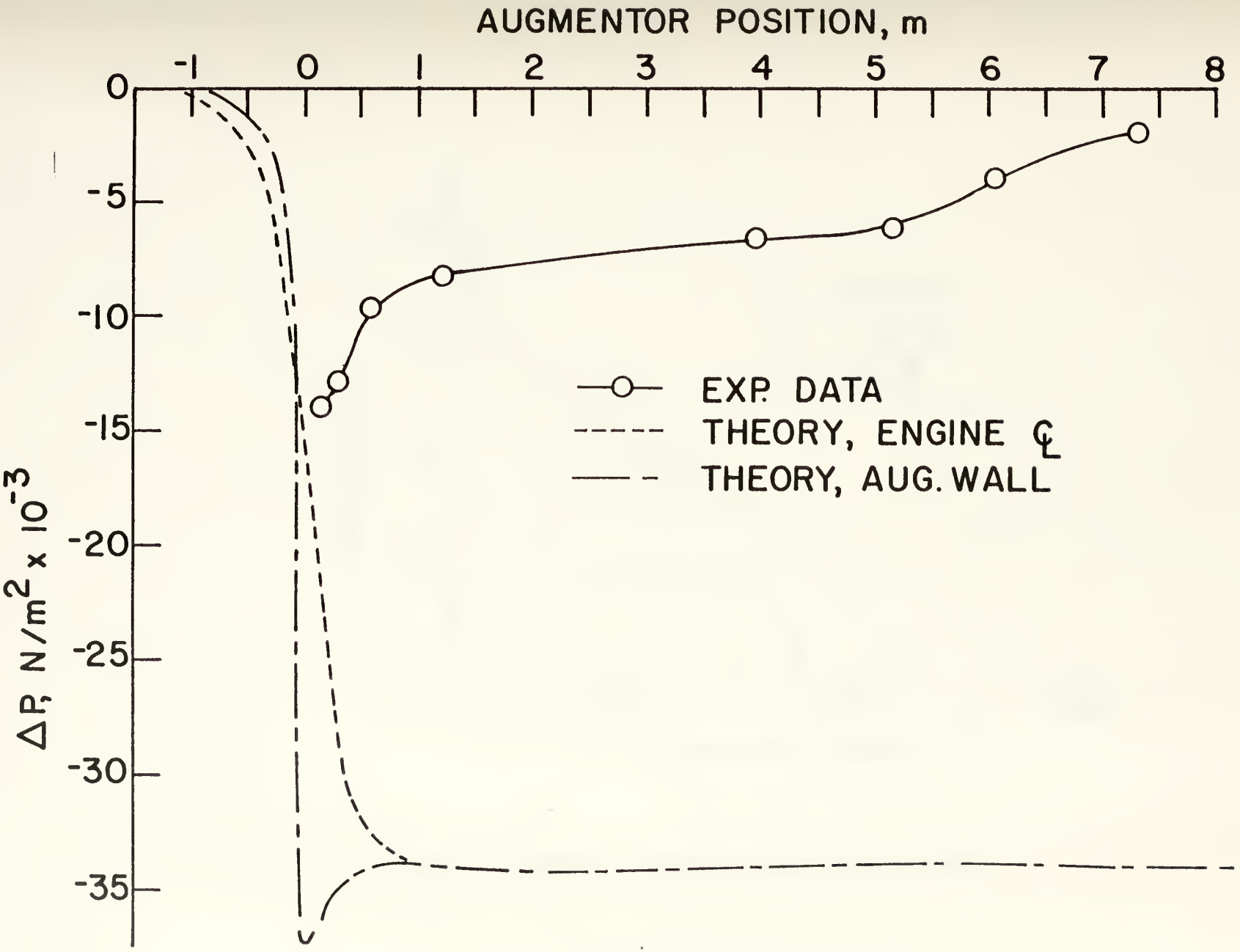

Fig. 12 Pressure Profile, 100% Power

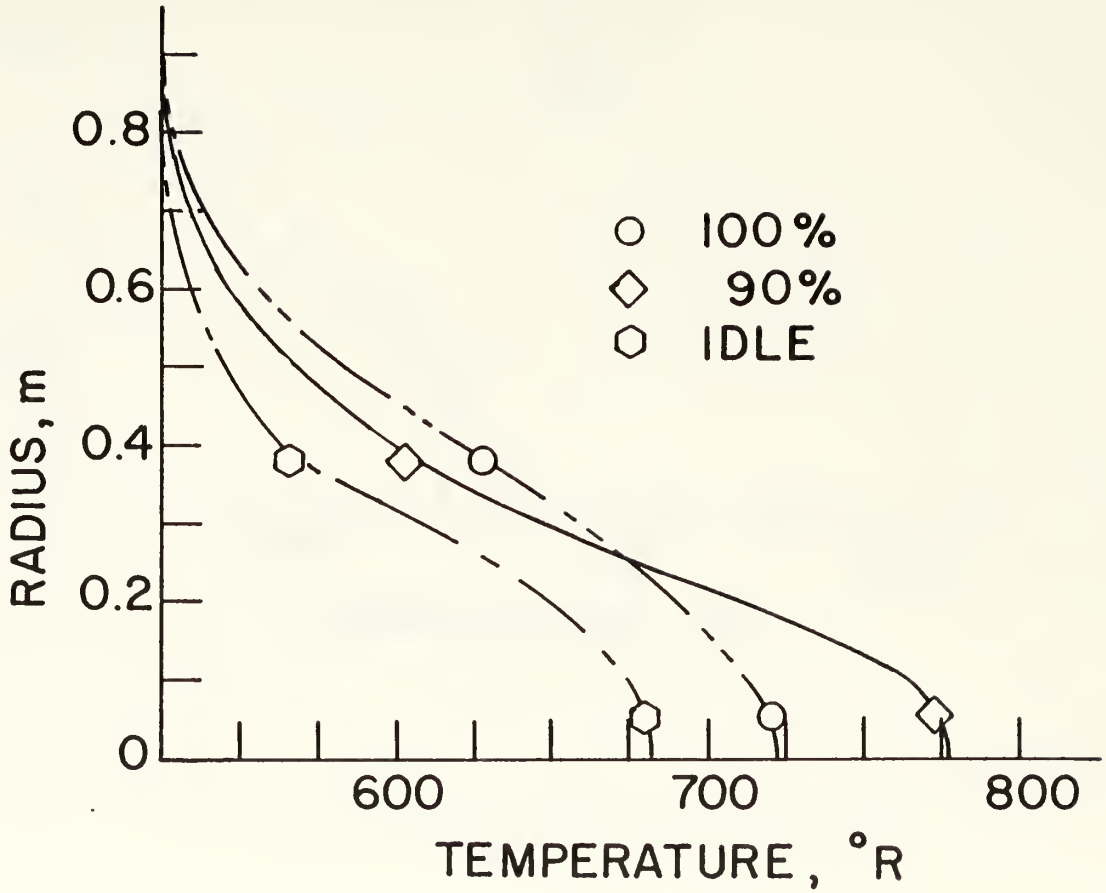

Fig. 13 Stagnation Temperature Profiles, Aft Rake

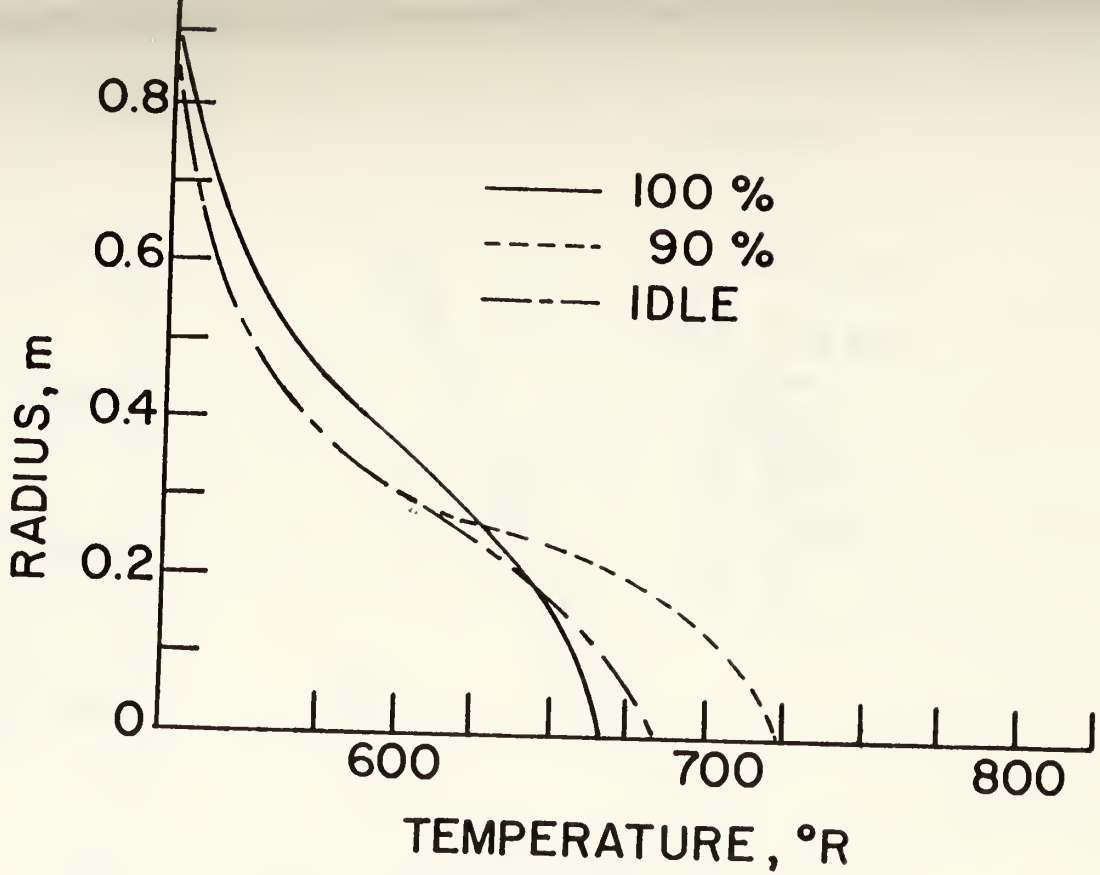

Fig. 14 Static Temperature Profiles, Aft Rake

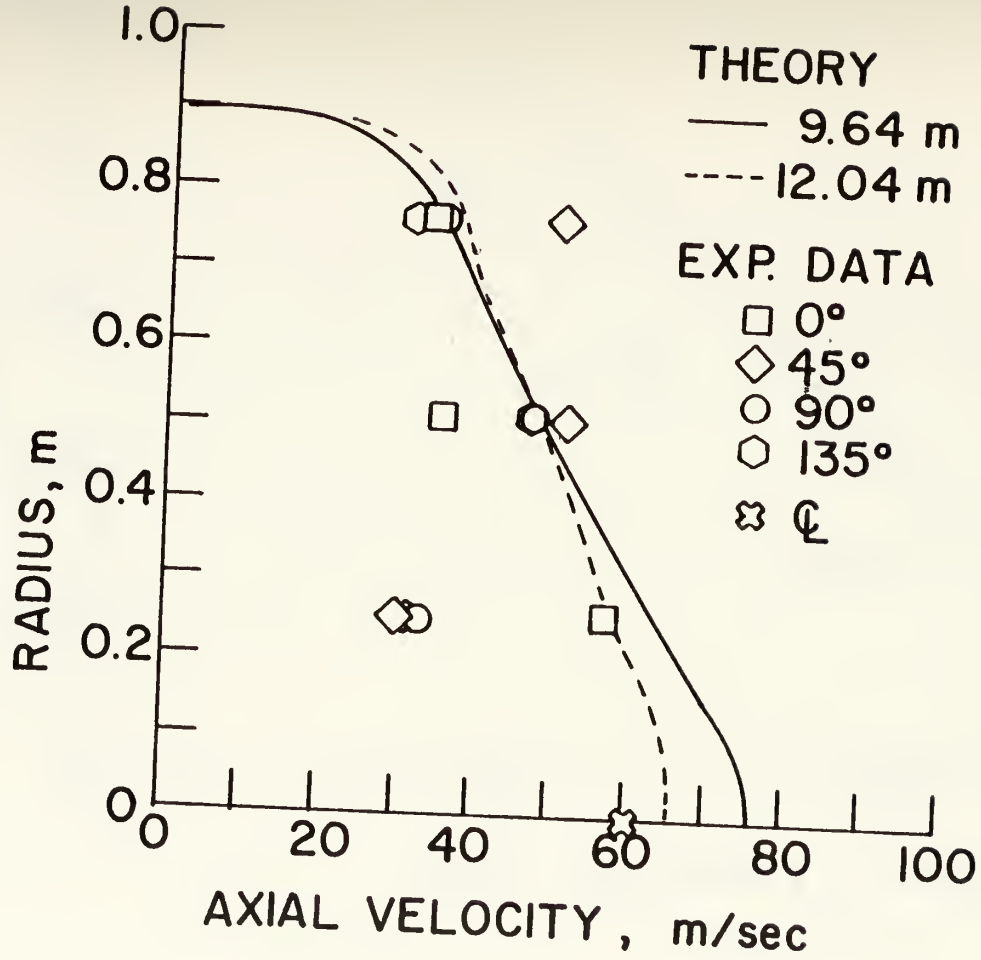

Fig. 15 Velocity Profile, Aft Rake, Idle Power

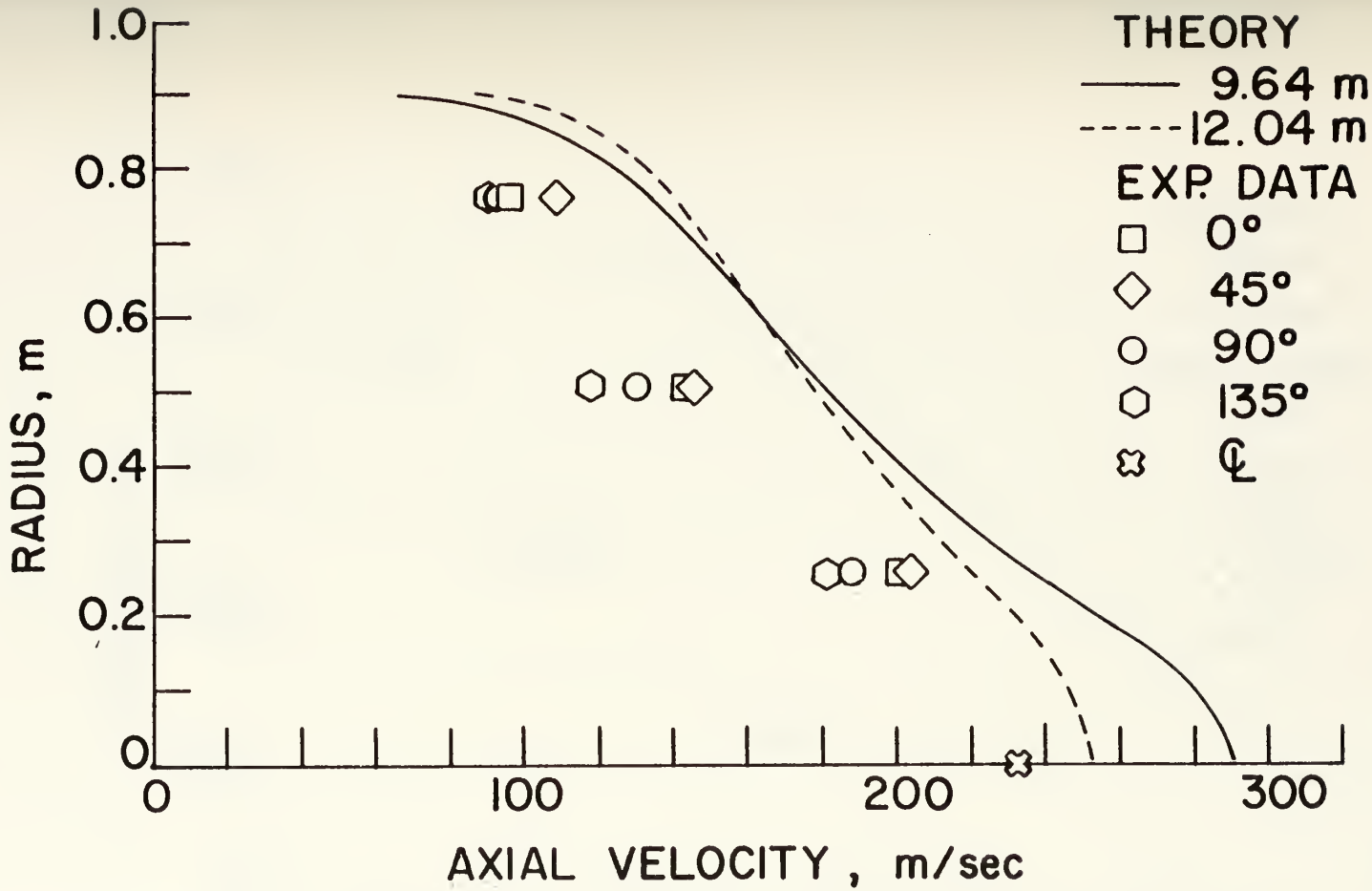

Fig. 16 Velocity Profile, Aft Rake, 90% Power

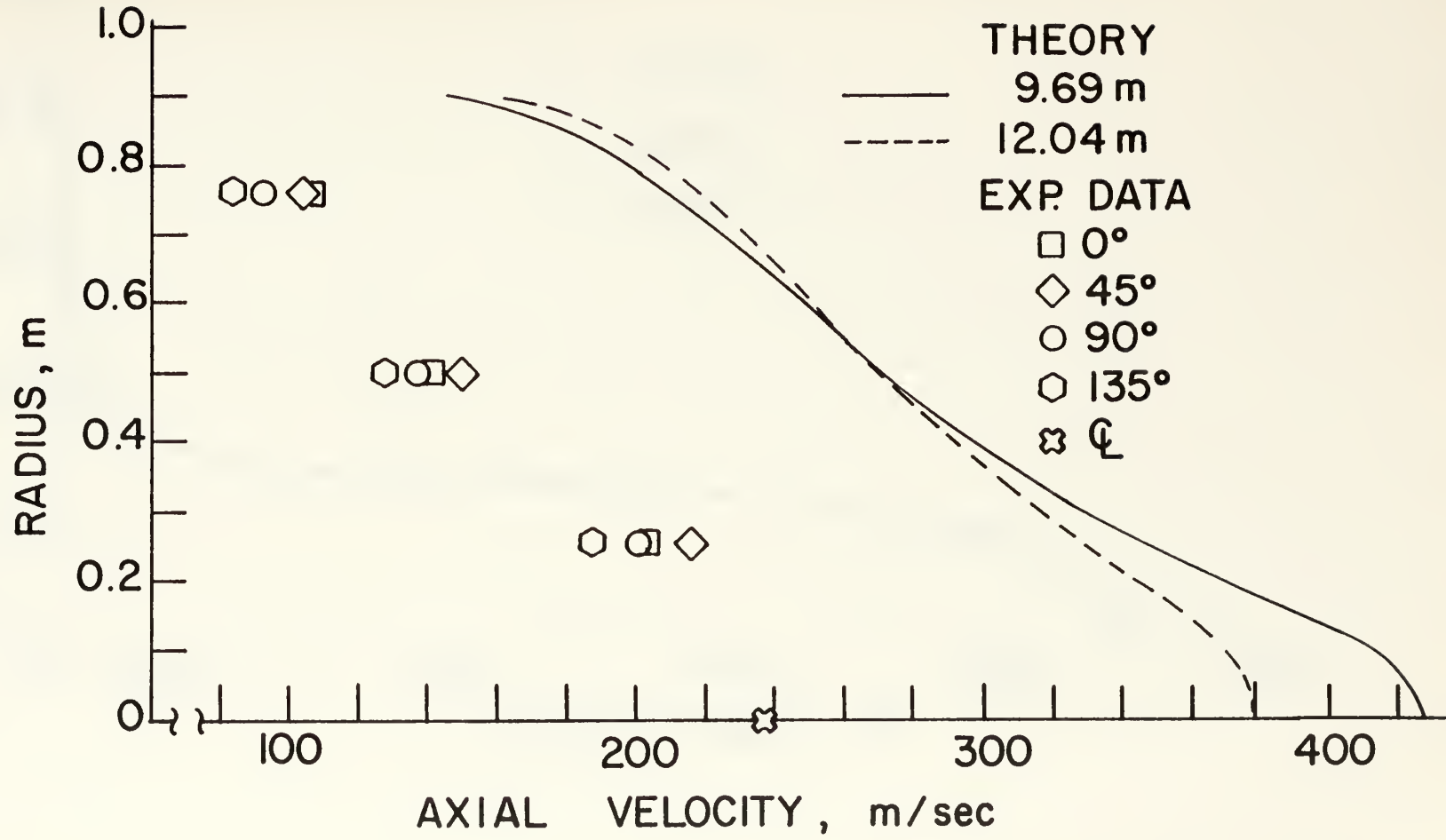

Fig. 17 Velocity Profile, Aft Rake, 100% Power

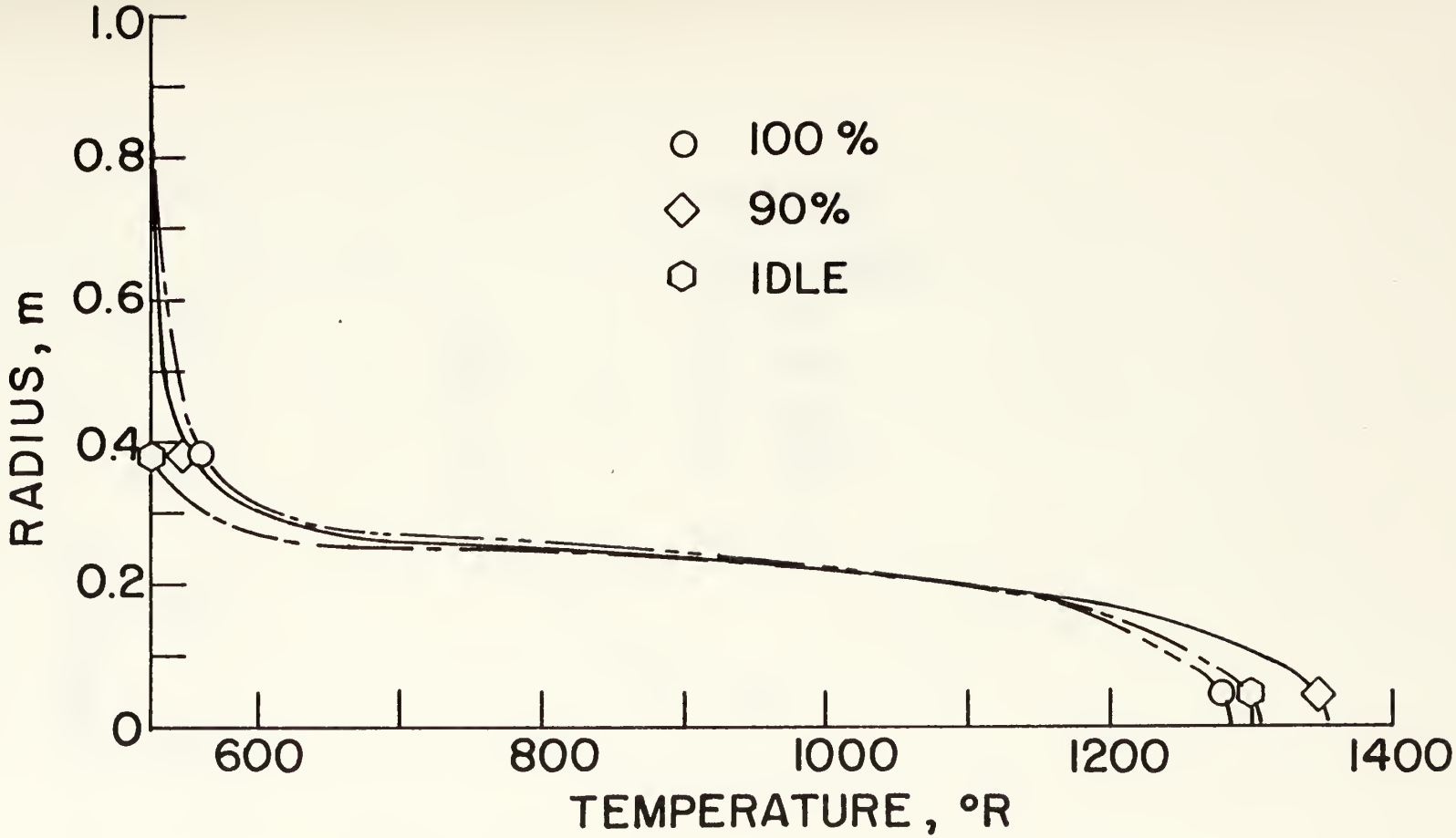

Fig. 18 Stagnation Temperature Profiles, Forward Rake

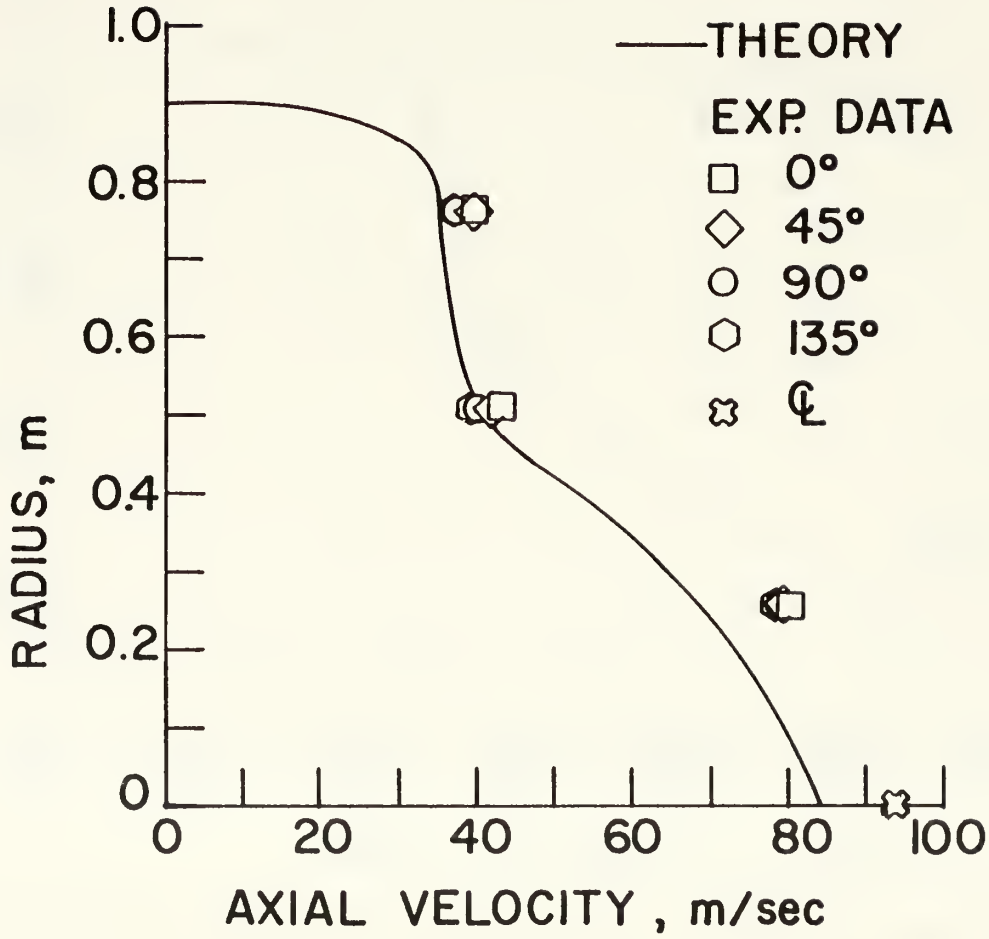

Fig. 19 Velocity Profile, Forward Rake, Idle Power

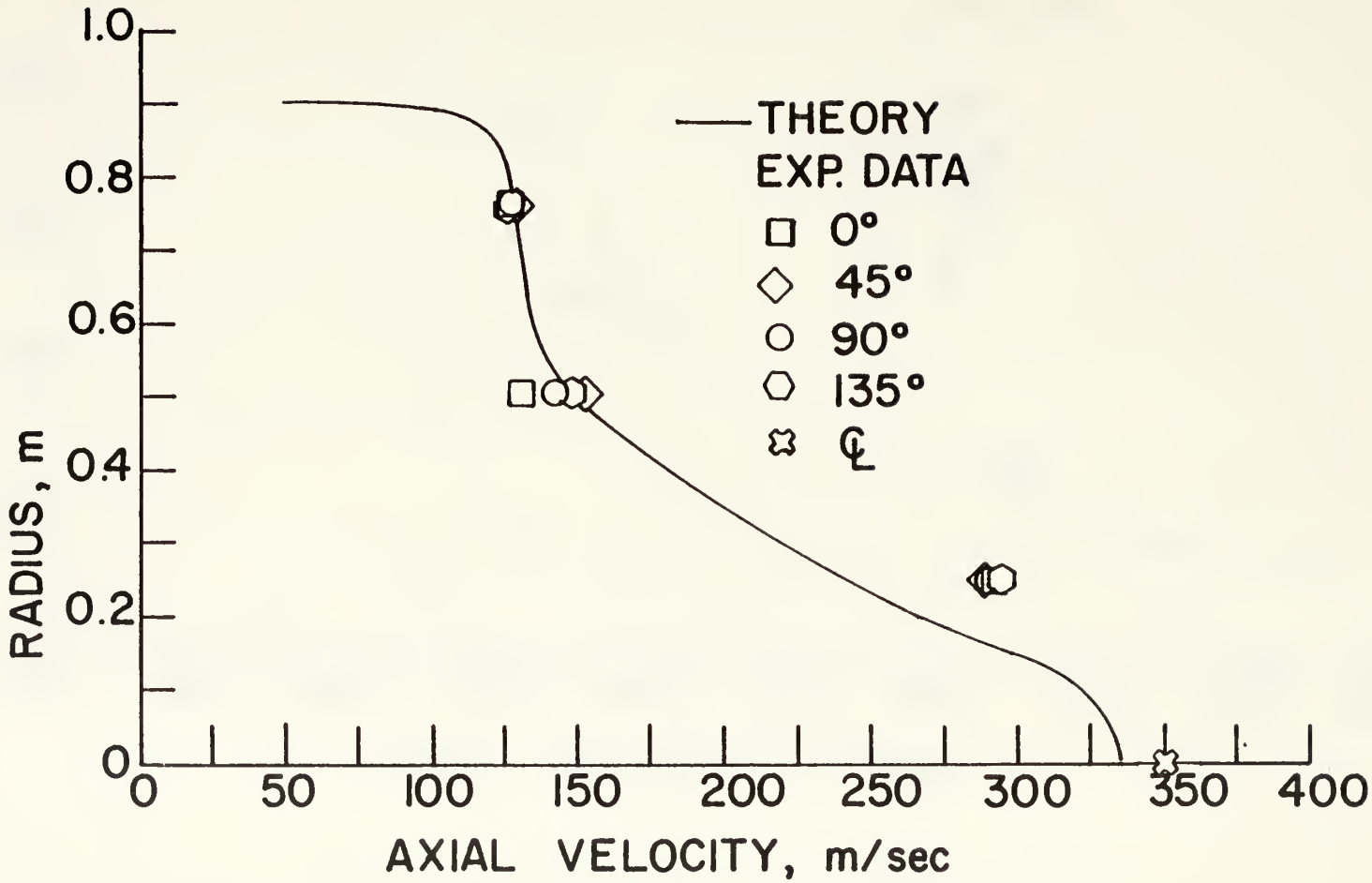

Fig. 20 Velocity Profile, Forward Rake, 90% Power

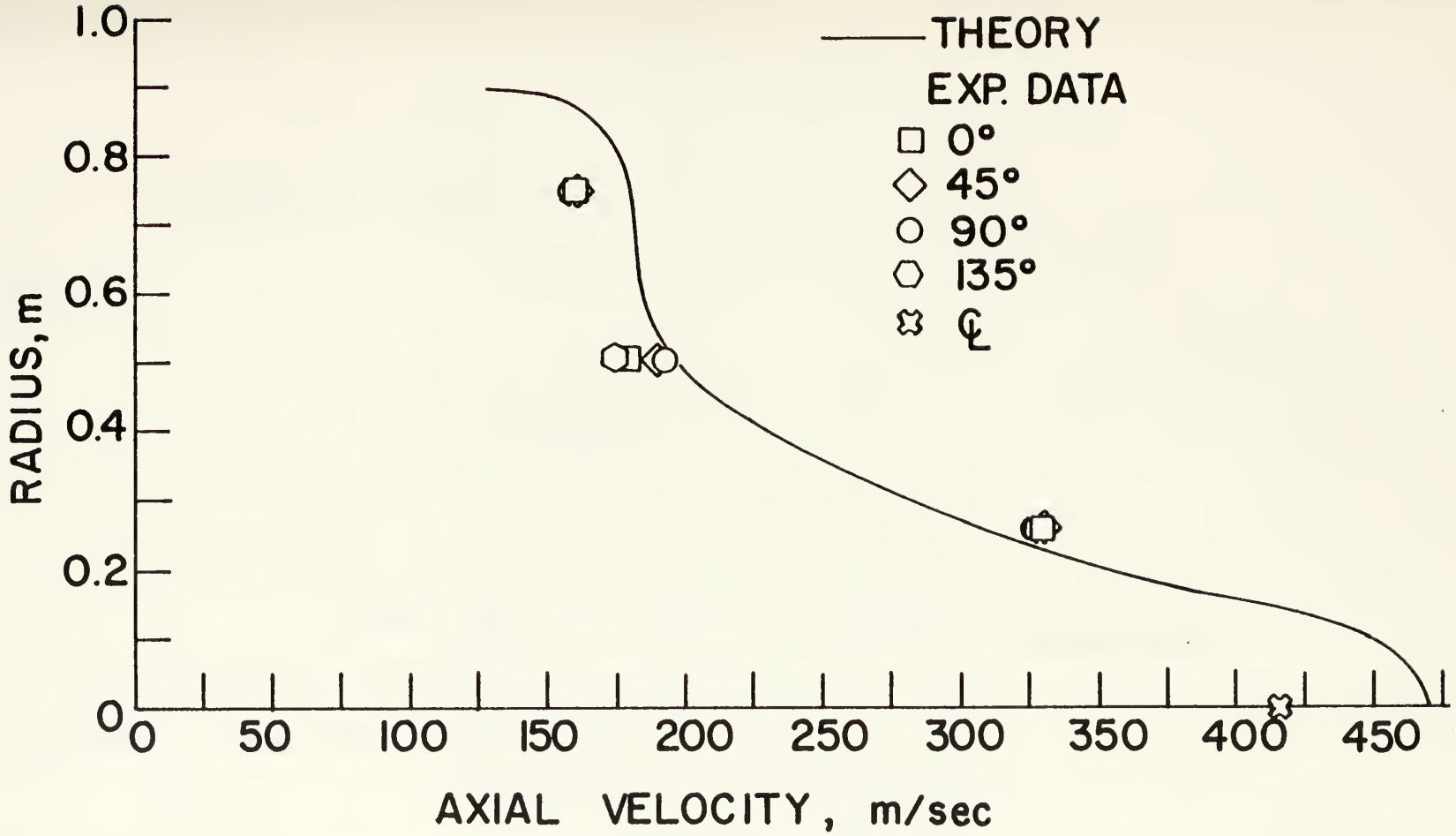

Fig. 21 Velocity Profile, Forward Rake, 100% Power

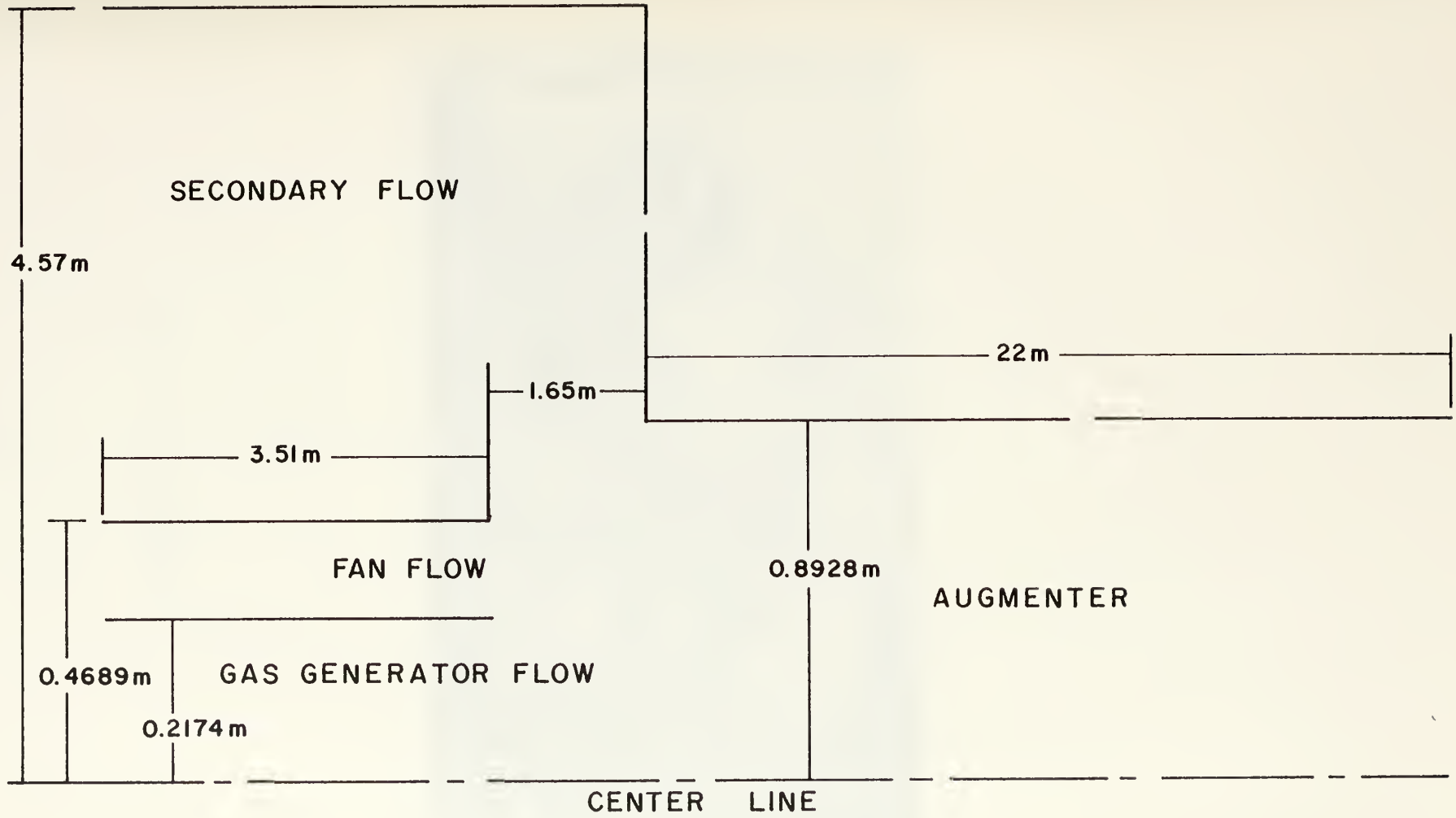

Fig. 22 Turbojet Test Cell Geometry for Computer Model

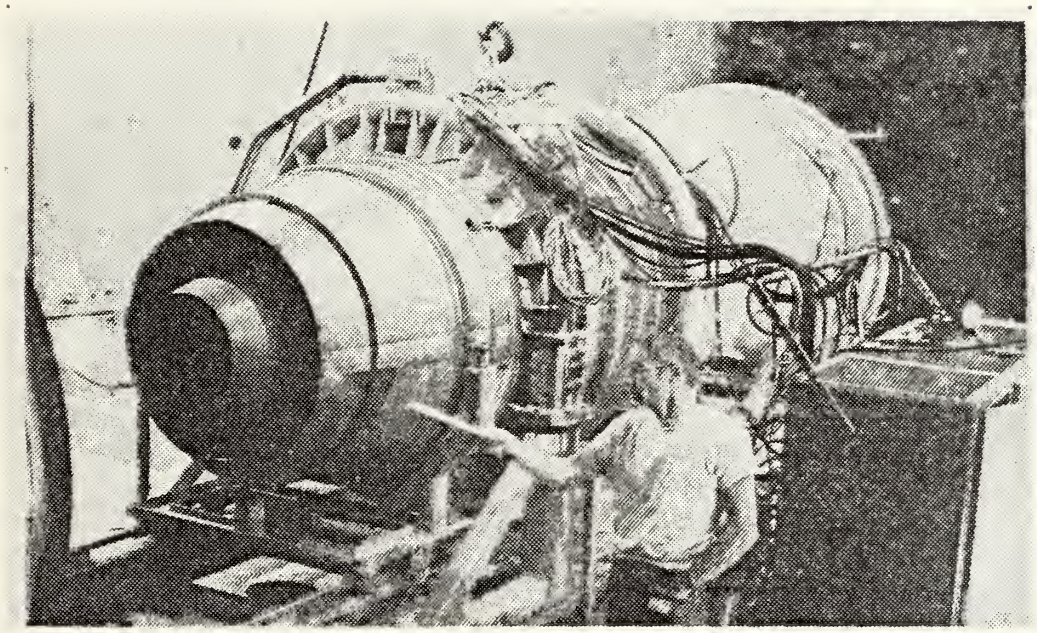

Fig. 23 TF-34 Exhaust

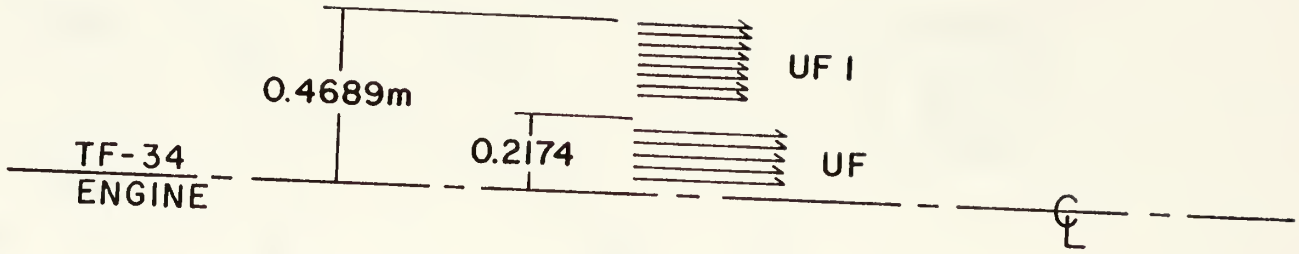

Fig. 24 Computer Model of TF-34 Exhaust Velocity Profile

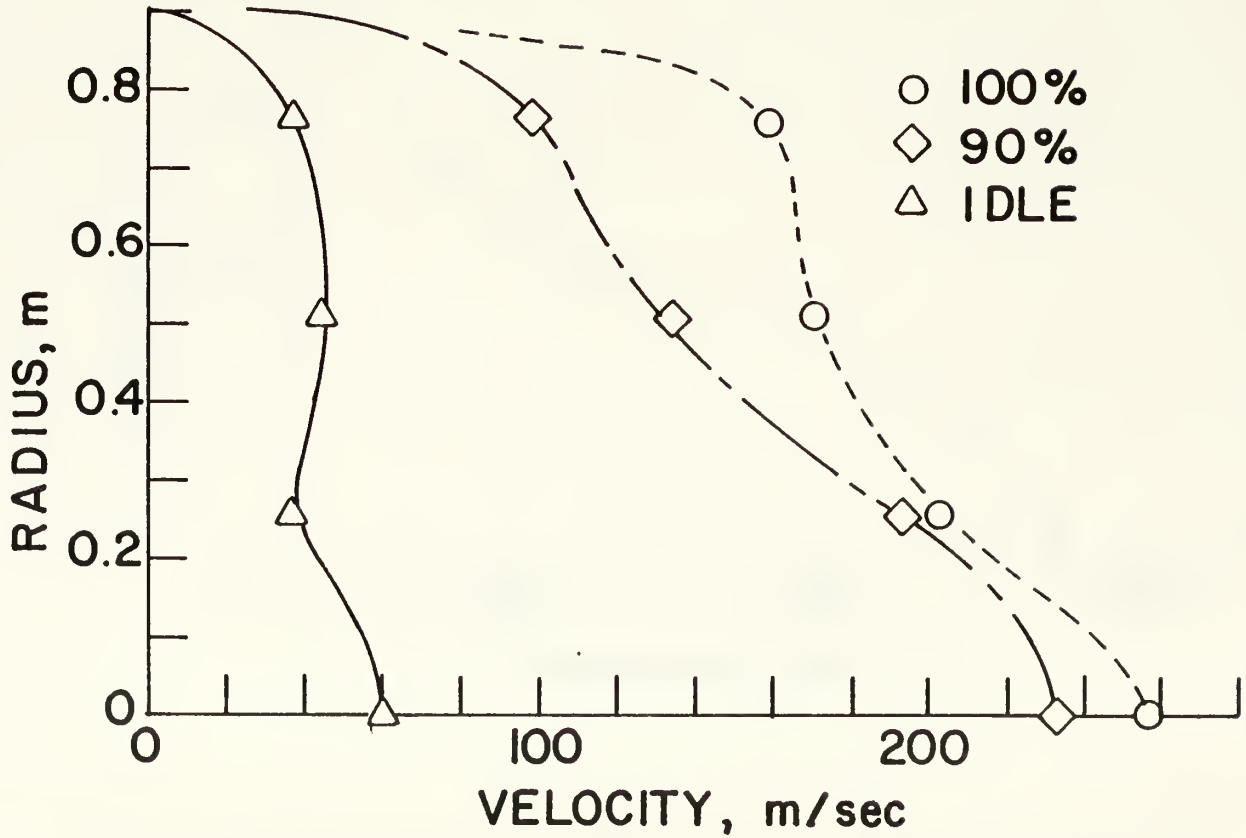

Fig. 25 Average Velocity Profiles, Aft Rake

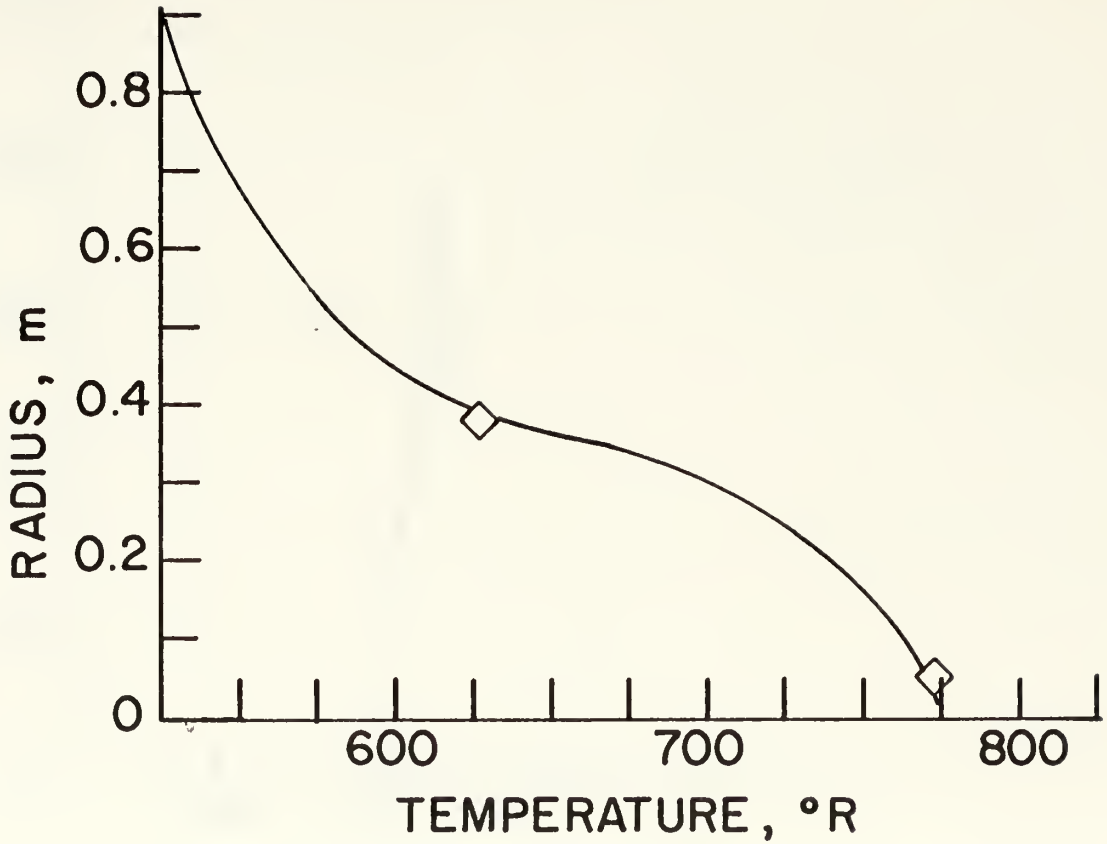

Fig. 26 Modified Stagnation Temperature Profile, Aft Rake, 90% Power

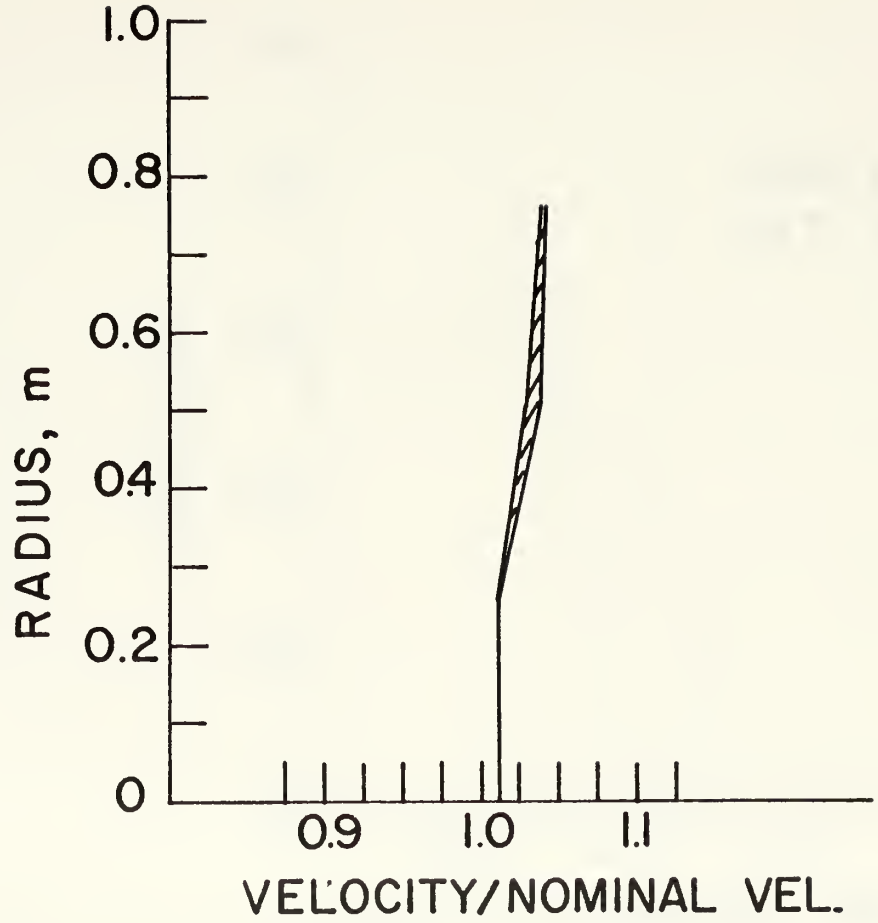

Fig. 27 Sensitivity of Velocity Profile to Uncertainties in Measured Static Pressure, 90% Power

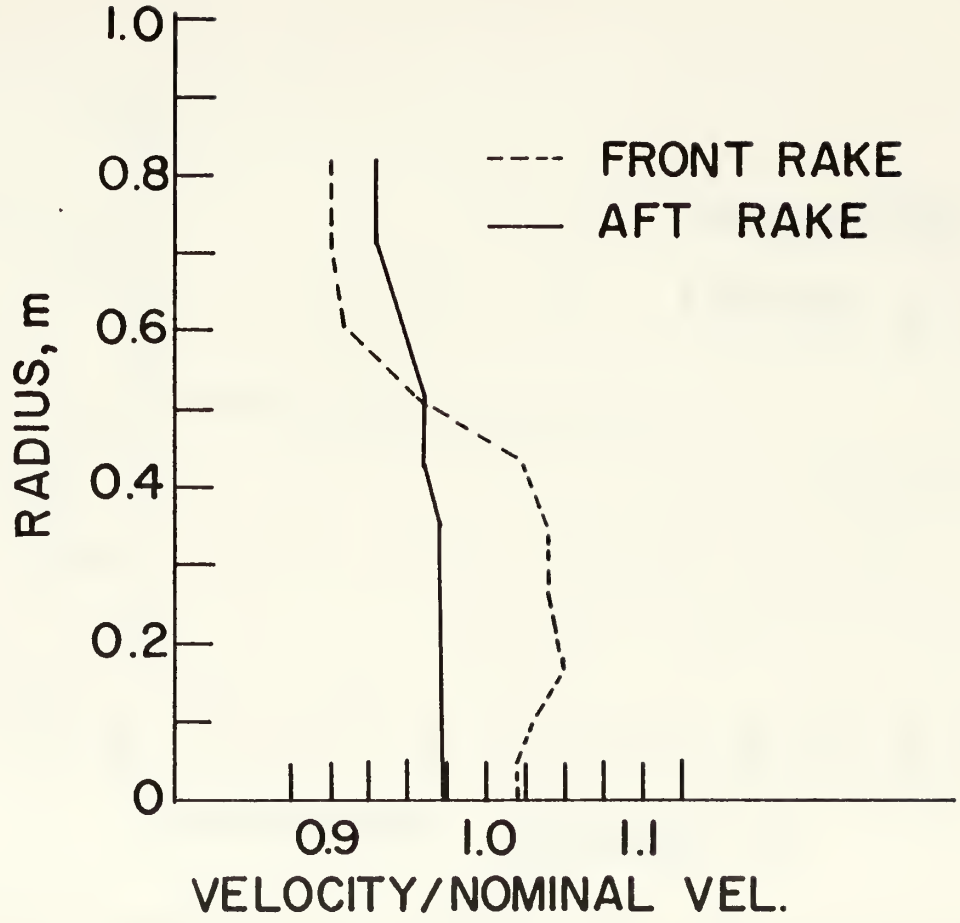

Fig. 28 Sensitivity of Predicted Velocity Profile to Test Cell Mass Flow Rate, 90% Power

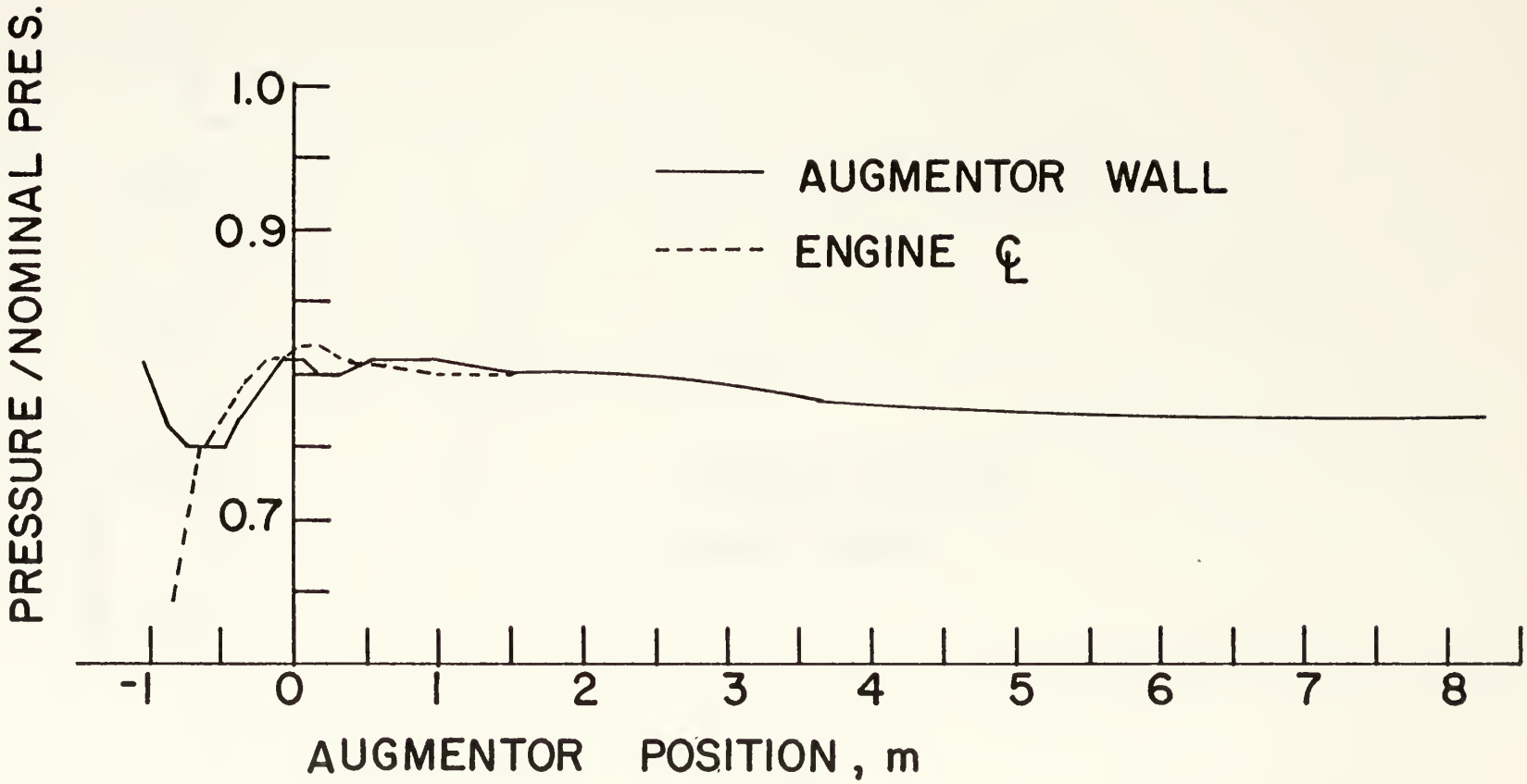

Fig. 29 Sensitivity of Predicted Static Pressure Profile to Test Cell Mass Flow Rate, 90% Power

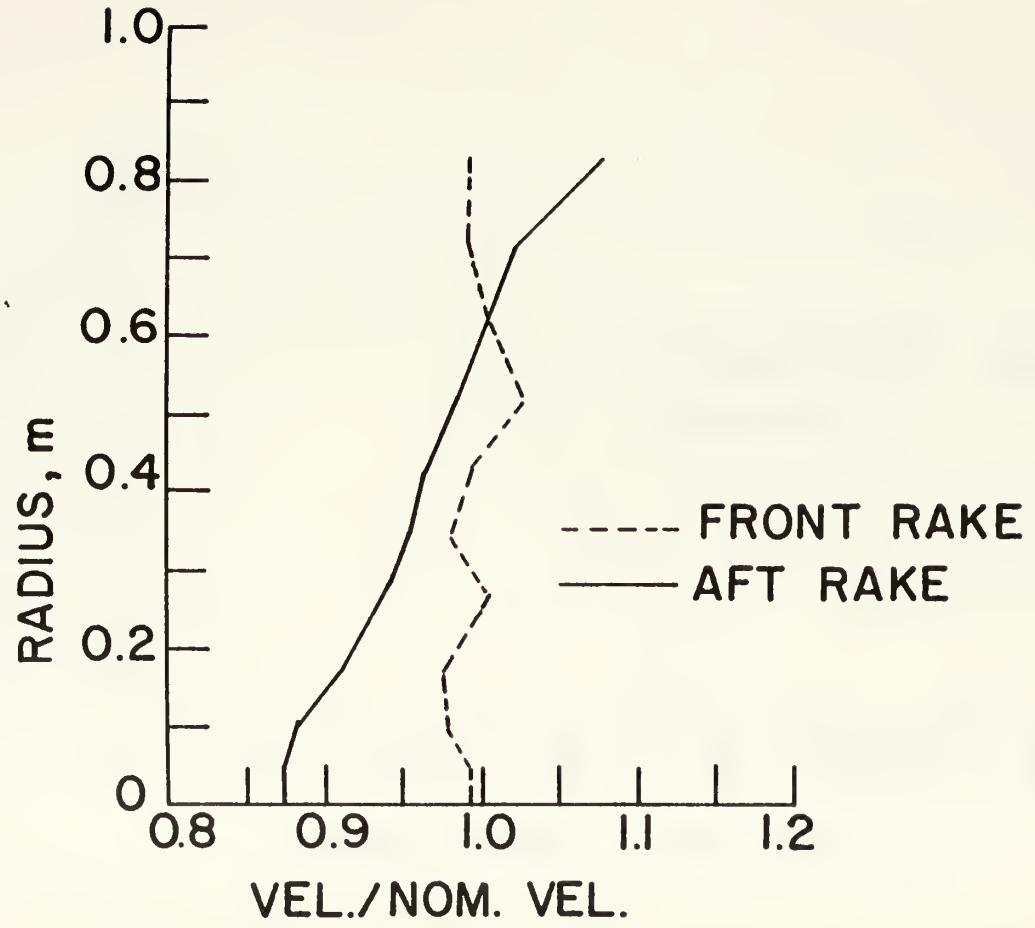

Fig. 30 Sensitivity of Predicted Velocity Profile to a 50% Increase in Effective Viscosity, 90% Power

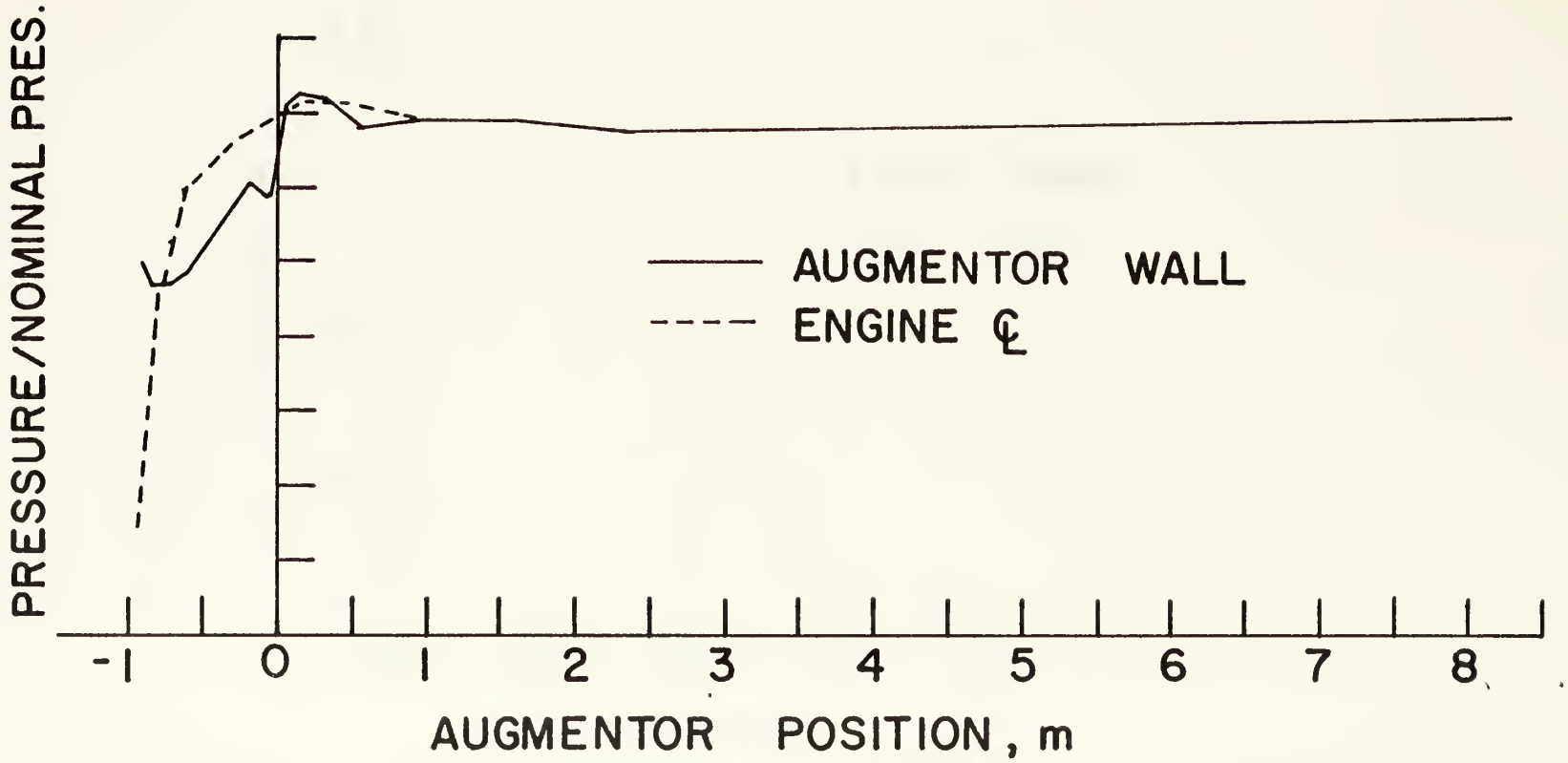

Fig. 31 Sensitivity of Predicted Pressure Profile to a 50% Increase in Effective Viscosity, 90% Power

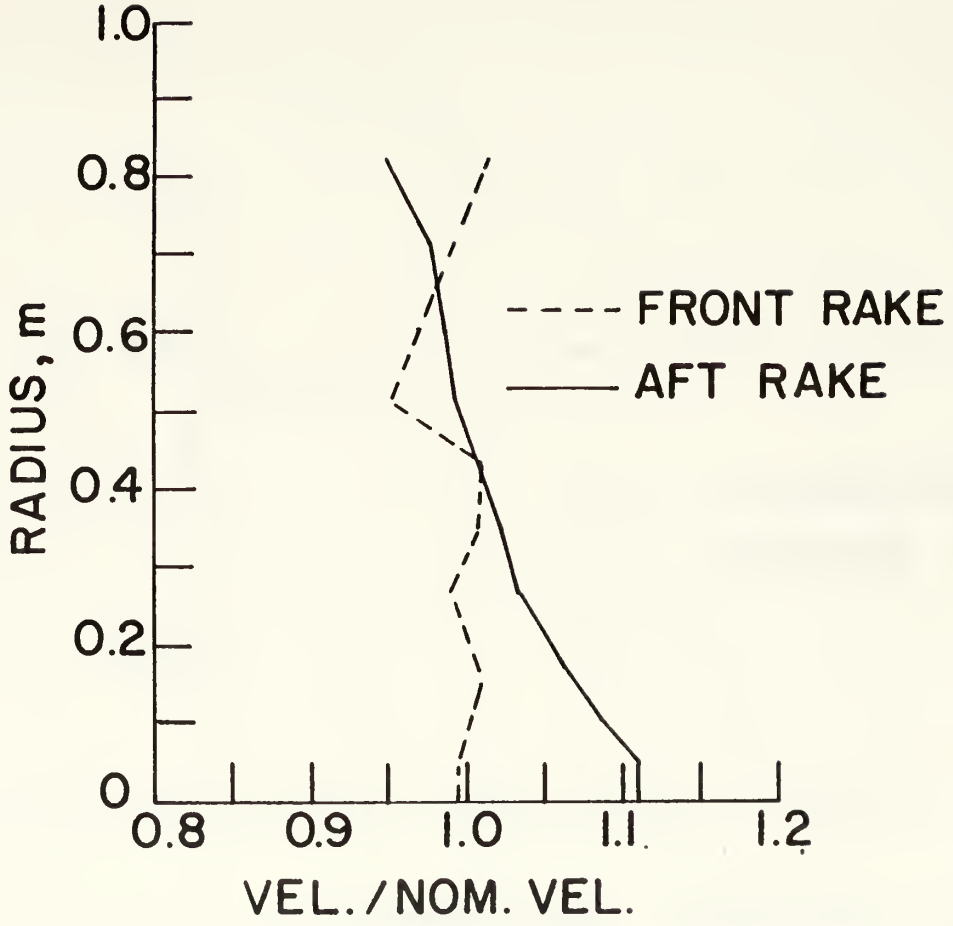

Fig. 32 Sensitivity of Predicted Velocity Profile to a 33% Decrease in Effective Viscosity, 90% Power

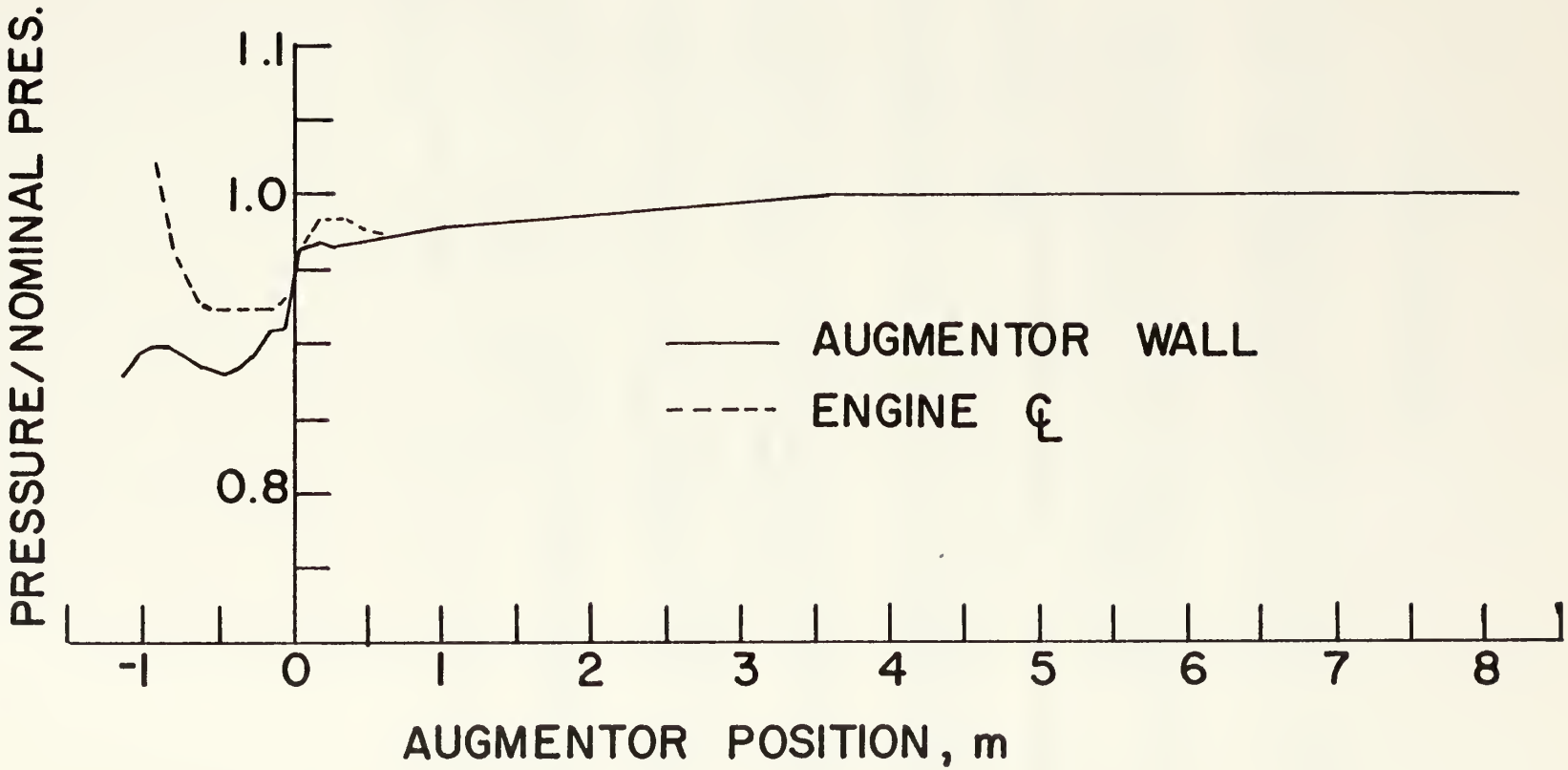

Fig. 33 Sensitivity of Predicted Pressure Profile to a 33% Decrease in Effective Viscosity, 90% Power

LIST OF REFERENCES

1. Stevenson, C. A. and Netzer, D. W., "A Primitive Variable Mathematical Model for Predicting the Flows in Turbojet Test Cells," Naval Postgraduate School Report Number NPS67-79-009, Monterey, CA., October, 1979.

2. Hayes, J. D. and Netzer, D. W., "An Investigation of the Flow in Turbojet Test Cells and Augmentors," Naval Postgraduate School Report Number NPS-57-Nt-75101, Monterey, CA., October 1975.

3. Gosman, A.D., and others, Heat and Mass Transfer in Recirculating Flows, Academic Press, 1969.

4. Spalding, D. B., Gosman, A. D., and Pun, W. M., The Predictions of Two-Dimensional Flows, Short Course, Pennsylvania State University, August, 1972.

5. Speakman, G. C., Hayes, J. D., and Netzer, D. W., "Internal Aerodynamics of Turbojet Test Cells," Naval Postgraduate School Report Number NPS-67Nt-76121, Monterey, CA., December 1976.

6. Walters, J. J. and Netzer, D. W., "A Validation of Mathematical Models for Turbojet Test Cells," Naval Postgraduate School Report Number NPS-67-78-002, Monterey, CA., June 1978.

7. Pun, W. M., and Spalding, D. B., "A General Computer Program for Two-Dimensional Elliptic Flows," Imperical College of Science and Technology, Report No. HTS/76/2, August 1977.

8. General Electric Aircraft Engine Group, TF-34 Installation Manual, Lynn, Mass., May 1971.

INITIAL DISTRIBUTION LIST

		No. Copies
1.	Defense Technical Information Center Cameron Station Alexandria, Virginia 22314	2
2.	Library, Code 0142 Naval Postgraduate School Monterey, California 93940	2
3.	Department Chairman, Code 67 Pl Department of Aeronautics Naval Postgraduate School Monterey, California 93940	1
4.	Assoc. Prof. D. W. Netzer, Code 67 Nt Department of Aeronautics Naval Postgraduate School Monterey, California 93940	2
5.	Lt. Paul Joseph Mallon USS Kitty Hawk (CV-63) FPO San Francisco 96634	2

Thesis
M27826
c.1

Mallon

189737

Validation of a two-dimensional primitive variable computercode for flow fields in jet engine test cells.

Thesis
M27826
c.1

189737

Mallon

Validation of a two-dimensional primitive variable computercode for flow fields in jet engine test cells.

thesM27826
Validation of a two-dimensional primitiv
3 2768 002 04227 7
DUDLEY KNOX LIBRARY